blood

American Society of Hematology
2021 L Street NW, Suite 900,
Washington, DC 20036
Phone: 202-776-0544 | Fax 202-776-0545
editorial@hematology.org

A Notch trans-activation to cis-inhibition switch underlies hematopoietic stem cell aging

Tracking no: BLD-2024-026505R2

Francesca Matteini (The Bellvitge Institute for Biomedical Research (IDIBELL), Spain) Roshana Thambyrajah (Institut Hospital del Mar d'Investigacions Mèdiques, Spain) Sara Montserrat-Vazquez (The Bellvitge Institute for Biomedical Research (IDIBELL), Spain) Sascha Jung (CIC bioGUNE-BRTA (Basque Research and Technology Alliance), 5Ikerbasque, Basque Foundation for Science, Spain) Alba Ferrer-Perez (The Bellvitge Institute for Biomedical Research (IDIBELL), Spain) Patricia Herrero Molinero (Institut Hospital del Mar d'Investigacions Mèdiques, Spain) Dina El Jaramany (The Bellvitge Institute for Biomedical Research (IDIBELL), Spain) Javier Lozano-Bartolomé (The Bellvitge Institute for Biomedical Research (IDIBELL), Spain) Eva Mejia-Ramirez (The Bellvitge Institute for Biomedical Research (IDIBELL), Spain) Jessica Gonzalez Miranda (Institut Hospital del Mar d'Investigacions Mèdiques, Spain) Antonio Del Sol (Luxembourg Centre for Systems Biomedicine (LCSB), University of Luxembourg, Luxembourg) Anna Bigas (Hospital del Mar Research Institute CIBERONC, Spain) Maria Carolina Florian (Stem Cell Aging Group, Regenerative Medicine Program, The Bellvitge Institute for Biomedical Research (IDIBELL), Spain)

Abstract:
Aged hematopoietic stem cells (HSCs) expand in clusters over time, while reducing their regenerative capacity and their ability to preserve the homeostasis of the hematopoietic system. The expression of Notch ligands in the bone marrow (BM) niche is essential for hematopoiesis. However, the impact of Notch signaling for adult HSC function and its involvement in HSC aging remains controversial. Here we show that Notch activation in young HSCs is not homogeneous, and it is triggered by sinusoidal expression of the Notch ligand Jagged2 (Jag2). Sinusoidal Jag2 deletion in young mice recapitulates the decrease in Notch activity observed in aged HSCs and alters HSC divisional symmetry and fate priming, promoting myeloid-biased HSCs (My-HSCs) expansion. Mechanistically, our data reveals that upon decreasing sinusoidal Jag2 expression, HSCs themselves upregulate Jag2, which cis-inhibits Notch signaling, resulting in the expansion of My-HSCs and in reduced hematopoietic regeneration. Collectively, these findings identify the crosstalk between BM niche-driven and HSC intrinsic features in regulating HSC fate priming and regenerative potential and reveal an extrinsic Notch trans-activation to intrinsic cis-inhibition switch underlying HSC aging.

Conflict of interest: No COI declared

COI notes:

Preprint server: No;

Author contributions and disclosures: Conceptualization: FM, MCF Methodology: FM, SM-V, EM-R, AF-P, DE-J, JL-B, PH-M, RT, JG-M, AB, SJ, AD Investigation: FM, SM-V, MCF Visualization: FM, PH-M, RT Funding acquisition: MCF Project administration: MCF Supervision: AB, MCF Writing - original draft: FM, SM-V, MCF Writing - review & editing: AB, MCF

Non-author contributions and disclosures: No;

Agreement to Share Publication-Related Data and Data Sharing Statement: The source data underlying Figs. 1-7 and Supplementary Data Figs. 1-7 is provided as a Source Data file. scRNA-seq data are deposited at GEO (accession numbers GSE197070 and GSE269953) and all experimental raw data and the code for the scRNAseq data analysis can be found at https://doi.org/10.34810/data1340.

Clinical trial registration information (if any):

A Notch Trans-Activation to Cis-Inhibition Switch in Hematopoietic Stem Cell Aging

Context of Research

Aged hematopoietic stem cells (HSC) expand in clusters, while their regenerative capacity is reduced. The crosstalk between extrinsic and intrinsic features contributing to HSC functional decline upon aging is still not completely clear.

Aim of This Study

Here, by imaging the interaction between HSCs and their niche in vivo, we investigated the crosstalk between intrinsic and extrinsic HSC phenotypes, focusing on Notch activity in HSC fate determination upon aging.

Findings

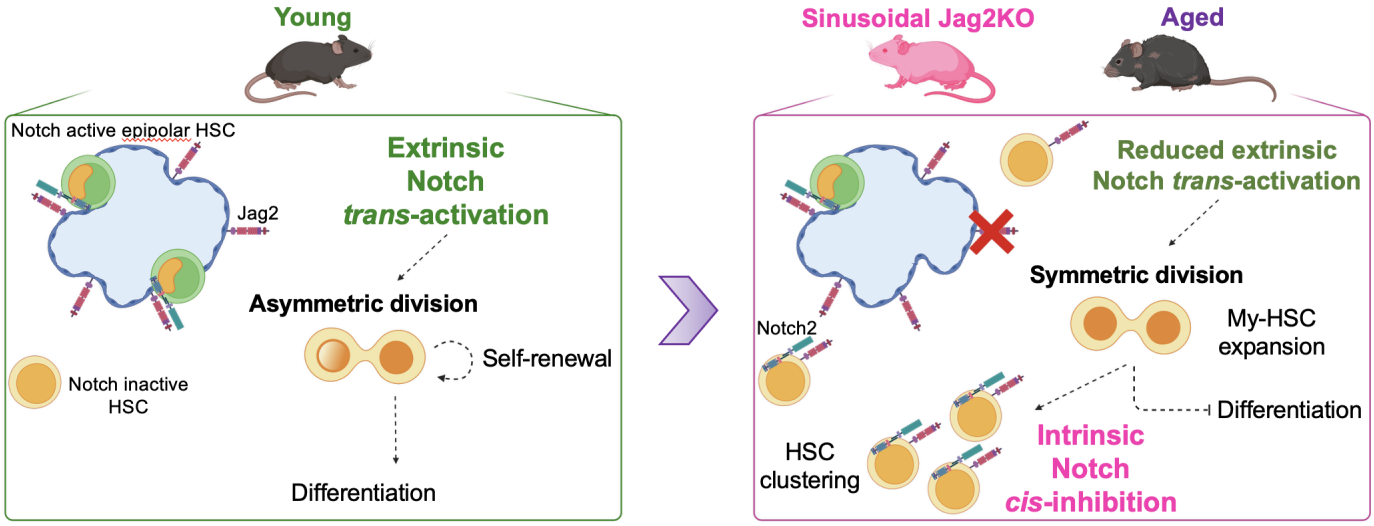

Conclusions: **In young HSCs, Notch activation is triggered by the sinusoidal expression of the Notch ligand Jagged2 (Jag2). As Jag2 expression in bone marrow sinusoids decreases with age, HSCs themselves upregulate Jag2, which cis-inhibits Notch signaling, resulting in the expansion of myeloid-biased HSCs and reduced hematopoietic regeneration.**

*Matteini et al. DOI: 10.xxxx/**blood**.2024xxxxxx*

blood Visual Abstract

A Notch trans-activation to cis-inhibition switch underlies hematopoietic stem cell aging

Francesca Matteini[1,2], Roshana Thambyrajah[3,4,5§], Sara Montserrat-Vazquez[1,2], Sascha Jung[6,7], Alba Ferrer-Perez[1,2], Patricia Herrero Molinero[3,4,5], Dina El Jaramany[1,2], Javier Lozano-Bartolomé[1,2], Eva Mejia-Ramirez[1,2,5], Jessica Gonzalez[3,4,5], Antonio Del Sol[6,7,8], Anna Bigas[3,4,5] and Maria Carolina Florian[1,2,5,9*]

[1]Stem Cell Aging Group, Regenerative Medicine Program, The Bellvitge Institute for Biomedical Research (IDIBELL), L'Hospitalet de Llobregat, Barcelona, Spain.

[2]Program for advancing the Clinical Translation of Regenerative Medicine of Catalonia, P-CMR[C], Barcelona, Spain

[3]Cancer Research Program, Institut Municipal d'Investigacions Mèdiques, (IMIM), Hospital del Mar, Barcelona, Spain

[4]Josep Carreras Leukemia Research Institute, Badalona, Spain

[5]Center for Networked Biomedical Research on Bioengineering, Biomaterials and Nanomedicine (CIBER-BBN) and cancer (CIBERONC), Madrid, Spain

[6]CIC bioGUNE-BRTA (Basque Research and Technology Alliance), Bizkaia Technology Park, Derio, Spain

[7]Ikerbasque, Basque Foundation for Science, Bilbao, Bizkaia, 48012, Spain

[8]Luxembourg Centre for Systems Biomedicine (LCSB), University of Luxembourg, L-4362 Esch-sur-Alzette, Luxembourg

[9]The Catalan Institution for Research and Advanced Studies (ICREA), Barcelona, Spain

§current address: Universidad de Cantabria, Facultad de Medicina, C/ Cardenal Herrera Oria, s/n. 39011 Santander; e-mail: roshana.thambyrajah@unican.es

*Corresponding author: M. Carolina Florian, Regenerative Medicine Program, Bellvitge Institute for Biomedical Research (IDIBELL), Barcelona, Spain; e-mail: mflorian@idibell.cat

Lead contact: Correspondence and requests for materials should be addressed to M. Carolina Florian, Regenerative Medicine Program, Bellvitge Institute for Biomedical Research (IDIBELL), Barcelona, Spain; e-mail: mflorian@idibell.cat

Data availability statement

The source data underlying Figs. 1-7 and Supplementary Data Figs. 1-7 is provided as a Source Data file. scRNA-seq data are deposited at GEO (accession numbers GSE197070 and GSE269953) and all experimental raw data and the code for the scRNAseq data analysis can be found at https://doi.org/10.34810/data1340.

Keypoints:

1. Notch activity decrease in HSCs induces myeloid-biased stem cell expansion and clustering at the expenses of hematopoietic regeneration

2. Deletion of sinusoidal Jag2 decreases Notch activity in HSCs, increasing symmetric divisions and impairing daughter fate commitment

Abstract

Aged hematopoietic stem cells (HSCs) expand in clusters over time, while reducing their regenerative capacity and their ability to preserve the homeostasis of the hematopoietic system. The expression of Notch ligands in the bone marrow (BM) niche is essential for hematopoiesis. However, the impact of Notch signaling for adult HSC function and its involvement in HSC aging remains controversial. Here we show that Notch activation in young HSCs is not homogeneous, and it is triggered by sinusoidal expression of the Notch ligand Jagged2 (Jag2). Sinusoidal Jag2 deletion in young mice recapitulates the decrease in Notch activity observed in aged HSCs and alters HSC divisional symmetry and fate priming, promoting myeloid-biased HSCs (My-HSCs) expansion. Mechanistically, our data reveals that upon decreasing sinusoidal Jag2 expression, HSCs themselves upregulate Jag2, which cis-inhibits Notch signaling, resulting in the expansion of My-HSCs and in reduced hematopoietic regeneration. Collectively, these findings identify the crosstalk between BM niche-driven and HSC intrinsic features in regulating HSC fate priming and regenerative potential and reveal an extrinsic Notch trans-activation to intrinsic cis-inhibition switch underlying HSC aging.

Introduction

HSCs constantly sustain blood and immune cells production throughout development, adulthood, and aging[1]. While during early phases of the hematopoietic development the proliferation and regenerative potential of HSCs is at the peak, over time HSC repopulation ability decreases[1–4]. Upon aging the HSC pool expands and shows a progressive myeloid differentiation skewing and an impaired regenerative capacity[5,6]. The BM microenvironment extensively regulates HSC differentiation and plays a critical role in the decline of stem cell function upon aging, contributing to the so-called *extrinsic* HSC aging[7–14]. A prominent role in driving extrinsic HSC aging is played for example by the remodeling of the bone marrow vasculature and by changes in adrenergic innervation, while sinusoids have been shown to protect HSCs from aging[9,15–18]. However, aging affects HSC function also independently from the old BM niche and *intrinsic* HSC aging is not rescued upon transplantation of old stem cells into a young BM microenvironment[3,5,19,20]. An intriguing phenotype of intrinsic HSC aging is HSC clustering[19]. In young mice, immediately after HSC division, daughter cells move far away from one another, and young HSCs are very rarely found close to each other. Upon aging, HSCs not only expand but are found in close proximity (within 19μm) to one another[16,19,21,22].

Notch signaling is a highly conserved evolutionary pathway controlling cell fate decision. In canonical situations, it occurs by cell-cell contact, where one cell, the signaling sending cell, expresses one of the Notch ligands and the other cell, the signaling receiving cell, expresses one of the Notch receptors[23,24]. In the hematopoietic system while *ex vivo* studies showed specific functions for different Notch receptors and ligands, conditional-null mouse models of Notch receptors failed to recapitulate *in vivo* the phenotype observed *ex vivo*[25], indicating the importance of studying this signaling within its physiological microenvironment. The current general consensus is that Notch signaling plays a key role in HSC emergence during development, but so far its

implications in adult hematopoiesis are controversial, because Notch activity has been deemed dispensable for adult hematopoiesis, while Notch ligands Jag1 and Jag2 are necessary to sustain hematopoiesis in homeostasis, regeneration and after myelosuppression[4,26–32].

Recently, it has been shown a novel role of Notch signaling in determining HSC fate during development[33]. Jag1-Notch1 cis-inhibition prevents cell cycle entry and differentiation in nascent aorta-gonad-mesonephros (AGM) stem cells, preserving their immature stem cell phenotype in hematopoietic clusters of the embryonic aorta[33].

Here, by imaging the interaction between HSCs and their niche *in vivo*, we investigate the crosstalk between *intrinsic* and *extrinsic* HSC phenotypes, focusing on Notch activity in HSC fate determination upon aging.

Materials and Methods:

For more information, see Supplementary Materials and Methods, available on the *Blood* website.

Mouse Models

Hes1p-2dEGFP mice were obtained from Dr. Kageyama R. (Kyoto University, Japan). VEGFR3Cre^{Mer} Jag2*fl/fl* mice were generated by crossing VEGFR3Cre^{Mer} mice[34] of pure C57/Bl6 background obtained from Dr. Ichise H., University of the Ryukyus with Jag2*fl/fl* mice already backcrossed into a pure C57/BL6 background obtained from Dr. Gridley T.[35].

Results

Notch activity in HSCs is not homogeneous and depends on BM localization.

To investigate Notch activity in HSCs, we took advantage of *Hes1p-2dEGFP* mice (**Figure S1a**), which express a destabilized EGFP reporter under the control of the Hes1 promoter. *Hes1* is a direct target of Notch and in this mouse model, the EGFP has a half-life of 2.5h allowing for the visualization of fast Notch activation-inactivation waves[39,40]. Notch activity is extremely important during the development of the hematopoietic system[41,42]. By flow cytometry and histology, a strong EGFP signal is indeed detectable in $CD31^{+}$c-Kit^{+} HSCs and $GFI1^{+}$ intra-aortic cluster of the AGM from *Hes1p-2dEGFP* mice compared to wild-type (WT) control (**Figure S1b-c**)[4]. Consistent with reflecting Hes1-associated Notch activity, the EGFP expression in AGM cells is reduced upon treatment with blocking antibodies against Dll4, Jag1 and Notch1 compared to the IgG isotype control (**Figure S1d**). While Notch signalling is essential for early HSC development, it is dispensable for the maintenance of adult bone marrow HSCs and is gradually downregulated already while HSCs progress toward E11.5[26]. In agreement, we detect a strong reduction in the reporter fluorescence signal by flow cytometry, with less than 1% of $EGFP^{+}$ cells in the BM and thymus of young adult (10–12-week-old) mice (**FigureS1e-g**). Arguing that flow cytometry might not be sensitive enough to detect Notch activity in adult HSCs, we opted for using a more sensitive technique, iFAST3D histology[36]. By using this approach, we could identify few $EGFP^{+}$ cells in the BM of young adult *Hes1p-2dEGFP* mice (**Figure S2a**). Interestingly, within the HSC population (HSCs are identified by the exclusive expression of CD150 and the absence of CD11b, B220, CD5, Gr-1, Ter-119, CD8a, CD48 and CD41 lineage markers and CD31 and CD144 endothelial markers expression) only a fraction of cells express the reporter gene, indicating that Notch signaling activation is not homogeneous within the HSC pool and it is possible to identify Notch inactive ($EGFP^{-}$) and Notch active ($EGFP^{+}$) HSCs (**Figure 1a**). Most HSCs in young adult mice have active Notch signaling (56,4% of total HSC pool) (**Figure 1b**). By measuring the distance of HSCs from the endosteum and the vessels (stained by CD31 and CD144 and discriminated between sinusoids

and arterioles by shape and orientation), the 3D BM images showed that Notch active HSCs display a very specific localization pattern being significantly closer to sinusoids (median distance of 7.9µm from the edge of the closest sinusoid) and arterioles (median distance 57.5µm from the edge of the closest artery) compared to Notch inactive HSCs (median distance of 18µm and of 85µm from the edge of the closest sinusoid and arteriole respectively) (**Figure 1c-f**). Moreover, Notch active HSCs are in proximity (<10µm) to sinusoids (56.7%), arteries (24.3%) or are close (<50µm) to the endosteum (27.3%), while Notch inactive HSCs have a general reduction in frequency of proximal localization to all niche structures (**Figure S2b**). The percentage of Notch inactive HSCs within 10µm (direct contact) from sinusoids is significantly less and Notch inactive HSCs are found very frequently (36.7% *vs* 1.3% for Notch active HSCs) in a non-specific localization, i.e. not proximal to sinusoids, arteries, or endosteum (**Figure S2b-c**).

Previously, we reported that the polarity of H4K16ac (epigenetic polarity or epipolarity) correlates with the regenerative capacity of stem cells and declines over time[16,19,43–45]. By iFAST3D histology, we measured a significant higher level of H4K16ac polarity for Notch active HSCs (>90%) (**Figure 1g-i**).

Collectively, these data indicate that Notch signaling activation is not homogeneous in adult HSCs and Notch active HSCs show a sinusoidal-specific localization associated to H4K16ac polarity, suggesting that these HSCs might represent the fraction of stem cells with the highest regenerative capacity.

Sinusoidal Jag2 regulates Notch activity and regenerative capacity of HSCs.

Previously, it was reported that in BM the Notch ligand Jag2 is mainly expressed by Nestin^{+} MSCs and endothelial cells and exerts an important role in regulating adult HSC function[16,31]. Since we detected that Notch active HSCs largely (>50%) localize close to sinusoids with a median distance

of less than one cell diameter (<10μm) suggesting a direct cell-cell contact (**Figure 1c-f** and **Figure S2b-c**), we wondered whether sinusoidal endothelial Jag2 affects Notch activity in HSCs. To address this point, we established a mouse model to selectively delete Jag2 in sinusoidal endothelial cells (SEC) by crossing *VEGFR3Cre*^{Mer} mice with *Jag2fl/fl* mice, hereafter referred as SEC^{Jag2KO} mice (**Figure 2a**)[34,46]. Upon administration of tamoxifen (TAM), in BM of SEC^{Jag2KO} mice, Jag2 is successfully deleted selectively at SEC (**Figure S3a-b**), without affecting the other Notch ligands like Delta4 (Dll4) and Jagged1 (Jag1) (**FigureS3c-d**). SEC Jag2 deletion mildly reduces sinusoidal volume, without affecting sinusoidal number and branching (**Figure S3e**) and it is not required to maintain HSPC function under homeostatic conditions in young adult mice, in agreement with previous reports[31] (**Figure S4a**). However, after myeloproliferative stress induced by a single 5-fluorouracile (5-FU) injection, SEC^{Jag2KO} mouse survival is significantly reduced. Necropsy analysis identified peritonitis and clear leucocytes infiltration in the peritoneum, in association with a transitory sharp expansion of white blood cells and increased reduction of hemoglobin 2 weeks after 5FU administration (**Figure 2b-d**).

Next, to evaluate whether sinusoidal endothelial Jag2 triggers Notch activation in HSCs, BM cells isolated from young *Hes1p-2dEGFP* mice were transplanted in lethally irradiated young SEC^{Jag2KO} mice alongside with littermate wild-type recipients. 6 weeks after transplantation, when the BM microenvironment has fully recovered from the preconditioning irradiation, Jag2 deletion was induced by tamoxifen treatment and mice were analyzed 7 days later (**Figure 2e**). The frequency of Notch active HSCs significantly decreases in SEC^{Jag2KO} recipients compared to controls (**Figure 2f**). Of note, sinusoidal Jag2 deletion reduces the fraction of Notch active HSCs in proximity to sinusoids, and these cells localize significantly further away from sinusoids (**Figure 2g-i**).

Interestingly, after Jag2 deletion, HSCs double in number, as observed by both flow cytometry (HSCs are gated as Lin$^-$c-Kit$^+$Sca-1$^+$Flt3$^-$CD34$^-$) and by iFAST3D (HSCs identified as Lin$^-$Cd48$^-$

Cd41^{-}Cd150^{+}; **Figure S4b-c**and **Figure 3a-b**), while epipolar HSCs are significantly reduced and their distance from sinusoids but not arterioles is significantly increased (**Figure 3c-e**). Increased activity of the small RhoGTPase Cdc42 in aged HSC has been correlated with loss of H4K16ac polarity in aged HSCs[43–45] and by western blot we observed increased Cdc42 activity upon SEC Jag2 deletion compared to WT controls (**Figure S4d**).

Next, to explore whether sinusoidal Jag2 deletion affects the intrinsic regenerative potential of HSCs, we performed serial competitive transplantations. Total BM cells from SEC^{Jag2KO} mice were transplanted in lethally irradiated young CD45.1^{+} recipients together with an equal amount of competitor BM cells (**Figure 3f**). Upon primary transplantation PB analysis over time does not show any significant alteration of SEC^{Jag2KO} engraftment, while revealing an increase of T cell and a decrease of Mac1+ cell frequency (**Figure 3g** and **Figure S5a-c**). In BM flow cytometry analysis shows a significant reduction in the engraftment of SEC^{Jag2KO} donor derived mice, together with an increase in HSCs and a decrease in lymphoid primed multipotent progenitors (LMPPs, gated as Lin^{-} c-Kit^{+}Sca-1^{+}Flt3^{+}CD34^{+}) frequency in the hematopoietic stem and progenitor compartment (gated as LSK, Lin^{-}c-Kit^{+}Sca-1^{+}) (**Figure 3h-i**and **Figure S5a**). Moreover, data shows a significant increase in common myeloid progenitors (CMPs, gated as Lin^{-}c-Kit^{+}Sca-1^{-}Fcg^{-}CD34^{+}), a decreased in granulocyte macrophage progenitors (GMPs, gated as Lin^{-}c-Kit^{+}Sca-1^{-}Fcg^{+}CD34^{+}) and confirmed the increase in T cell frequency (**Figure S5c-d**). Upon secondary transplantation, we detected a sharp drop in SEC^{Jag2KO} engraftment in PB with no alterations in HSC differentiation output (**Figure 3g** and **Figure S5e**). BM flow cytometry analysis confirmed the sharp reduction of SEC^{Jag2KO} engraftment, with a decrease in ST-HSC and an increase in CLP and Gr1^{+} cell frequency (**Figure 3j-k** and **Figure S5f-g**).

In conclusion, endothelial Jag2 deletion affect the sinusoidal volume in steady state and impairs recovery from myeloablative treatment, as also previously suggested[31]. Moreover, SEC^{Jag2KO}

reduces Notch activation in HSCs, and this is associated with reduced HSC epipolarity and quiescence, with displacement of HSCs away from the sinusoidal endothelial compartment and with decreased long term regenerative capacity of HSCs.

Deletion of sinusoidal Jag2 increases symmetric HSC divisions impairing daughter fate commitment.

Intrigued by the doubling of HSCs shortly after Jag2 deletion, we analyzed SEC^{Jag2KO} mice 24-28hrs after induction of Jag2 deletion (**Figure 4a** and **Figure S6a**) and at this time point we detected a sharp increase in the number of HSC dividing pairs (DP) (**Figure 4b-c**). Since we previously reported that the asymmetry of HSC division is linked to stem cell polarity[19], and in SEC^{Jag2KO} HSCs H4K16ac polarity decreases (**Figure 3c**), we scored asymmetric and symmetric HSC divisions by quantifying the amount of H4K16ac in paired daughter cells. The amount of H4K16ac distribution was measured on the major cell division plane of the DP, and H4K16ac inheritance in the daughter cells was determined by measuring the area underneath the curve of H4K16ac intensity in the daughter cells of the DP. Asymmetric divisions were defined by one daughter cell inheriting more H4K16ac compared to the other one (ratio between area curve intensity <0.65). When a similar amount (ratio between area curve intensity >0.65) of H4K16ac was detected between the 2 daughter cells, the division was scored as symmetric (**Figure 4b**). Data shows that compared to wild-type mice, where HSC divisions are infrequent and are mainly asymmetric, the number of H4K16ac symmetric divisions is selectively and significantly increased in SEC^{Jag2KO} mice (**Figure 4d**).

Next, to investigate whether the increased divisional symmetry was associated to a change in the outcome of daughter fate, we transplanted *Fgd5ZsGreen-TdTomato* HSCs into SEC^{Jag2KO} mice. In this experimental setting, donor HSCs are selectively label with the ZsGreen, which is under the

control of the *Fgd5* promoter and their progeny can be lineage traced by imaging TAM-inducible expression of TdTomato[47]. 6 weeks after transplantation, when the effect of the irradiation is overcome and the BM microenvironment has returned to its physiological conditions, Jag2 deletion in sinusoidal endothelial cells and TdTomato expression in HSCs were contemporary induced by TAM treatment. After induction, lineage tracing of HSC differentiation output was followed by PB flow cytometry analysis every 4 weeks, while iFAST3D BM histology to quantify HSPCs was performed at 24 hours and 7 days after treatment (**Figure 4e**). At 24 hrs after TAM, only HSCs brightly expressing ZsGreen ($ZsGreen^{bright}$) and positive for TdTomato ($TdTomato^{+}$) were detectable together with a few HSC DPs in which daughter cells were equally $ZsGreen^{bright}TdTomato^{+}$ in both WT and SEC^{Jag2KO} recipient mice. This data is suggestive of the existence of a differentiation priming rather than an alteration of cell fate commitment at such an early stage (**Figure 4f**). 7 days after TAM induction, it was possible to identify 5 subsets of $TdTomato^{+}$ cells. In agreement with previous reports[47,48], in *bona fide* we associated the different cell subsets to different stages of hematopoietic stem and progenitor cell differentiation. $ZsGreen^{bright}TdTomato^{+}$ and Exclusion Markers negative (EM^{-}) cells were identified as HSCs. Since the EM staining includes CD41 together with other lineage markers, we reasoned that $ZsGreen^{bright}TdTomato^{+}EM^{+}$ cells might be myeloid biased HSCs (My-HSCs) characterized by CD41 expression[49].$ZsGreen^{dim}TdTomato^{+}EM^{-}$ cells were identified as early committed progenitors (eProg), $ZsGreen^{-}TdTomato^{+}EM^{-}$ cells were associated to committed progenitors (cProg) and $ZsGreen^{-}TdTomato^{+}EM^{+}$ cells were defined as early differentiated cells (Diff) (**Figure 4e** and **Figure S6b-f** and **Supplementary videos SV_01 and SV_02**). The analysis reveals an increased frequency of My-HSCs in SEC^{Jag2KO} mice compared to WT, while HSCs are not affected (**Figure 4g-h** and **Figure S6c** and **Supplementary videos SV_03 and SV_04**). Of note, sinusoidal Jag2 knock-out increases clustering of the My-HSCs fraction (**Figure 4i**). eProg frequency is not affected

by sinusoidal Jag2 deletion, which instead strongly reduces cProg frequency (**Figure 4j-k** and **Figure S6h-i**). Importantly, PB lineage tracing analysis of HSC differentiation output at longer time point by flow cytometry indicates that in SEC^{Jag2KO} mice differentiation capacity of HSCs is significantly impaired, resulting in a reduction in all differentiated cell production in PB (**Figure 4l-m** and **Figure S6l** and **Supplementary videos SV_05 and SV_06**).

Collectively, these results suggest that sinusoidal Jag2 deletion induces an increase of symmetric HSC divisions, which is associated to an alteration in the fate of daughter cells characterized by an expansion of clustering My-HSCs and a reduction in committed progenitor output, supporting the impairment in regenerative capacity as measured by competitive transplantations.

Jag2 cis-inhibits Notch activity in aged HSCs

Notch signaling is suggested to be important for driving aging phenotypes but in many tissues, including the hematopoietic system, its function upon aging is so far poorly characterized[50,51]. To gain insight into a possible role of Notch signaling upon HSC aging, we analyzed aged (>80-week-old mice) *Hes1p-2dEGFP* mice. The data shows that most aged HSCs do not express the reporter gene (Notch inactive HSC) (**Figure 5a**) and the amount of Notch inactive HSC significantly increases upon aging (**Figure 5b**). To note all HSCs express Notch receptor 2 (Notch2) and a few HSCs (~2%) express also Notch1 (**Figure S7a-c, k)** suggesting that the reduction in Notch activity depends on a decrease in Notch trans-activation rather than on changes of Notch receptors expression.

Accordingly, aged Notch active HSCs are exclusively found close to sinusoids, while aged Notch inactive HSCs are significantly further away from sinusoids (**Figure 5c-e** and **Figure S7d**). Moreover, like in young mice, also in aged *Hes1p-2dEGFP* mice Notch active HSCs are mainly

epipolar and are closer to sinusoids and endosteum compared to Notch inactive HSCs (**Figure S7e-g**).

HSC clustering is an intrinsic phenotype characteristic of aged HSCs, where two or more HSCs are found in close proximity (<19mm) to each other[16,17,19,21,22]. In aged *Hes1p-2dEGFP* mice, HSC clustering is generally increased, and mainly aged Notch inactive HSCs are found closer to each other and more in cluster compared to Notch active HSCs (**Figure 5f-h**).

Interestingly, while we previously reported a significant decrease of Jag2 expression in aged Nes-GFP^{high} cells and at arteriolar endothelial BM cells[16], we observed now that aged HSCs themselves express Jag2 (**Figure 5i**) and that the frequency of Jag2^{+} HSCs significantly increases upon aging (**Figure 5j**). Increased Jag2 expression in aged HSCs correlates with HSC clustering, as Jag2^{+} HSCs are closer to one another and more clustered compared to the negative counterpart (**Figure 5k-l**). To understand whether HSC clustering is regulated by endothelial Jag2, we measured the distribution of HSCs in SEC^{Jag2KO} mice. Data shows a decrease in the minimum distance between HSCs and an increased HSC clustering in SEC^{Jag2KO} mice, correlated to an increased number and frequency of Jag2 expressing HSCs (**Figure 5m-o**). To further dig into Jag2^{+} HSCs, we pooled and interrogated our recently published scRNA-seq datasets from young and aged mice[45,52]. Cell annotation was done manually based on the cluster's marker genes and by using previously published signatures (**Figure 6a**, **Figure S7h-i** and **Supplementary Table 1**). Jag2^{+} cells were mainly found in the HSC cluster, both in young and aged mice (**Figure 6b**). Differential gene expression analysis comparing Jag2^{+} *vs* Jag2^{-} HSCs showed 26 differentially expressed genes (18 up- and 8 down-regulated genes; **Figure 6c** and **Supplementary Table 2**). Gene set enrichment analysis (GSEA) showed a significant positive enrichment of the aging signature defined by Svendsen et al[54]. in Jag2^{+} HSCs, as well as of the low-output signature defined by Rodriguez-Fraticelli et al.[55], while the high-output signature was significantly decreased (**Figure 6d**).

Furthermore, the myeloid-biased HSC signature described in Mann et al.[56] was positively enriched in Jag2$^+$ HSCs and the non-myeloid-biased HSC signature was significantly downregulated (**Figure 6d**). Dll4 and Jag1 are expressed at low level in HSCs and their expression is not changed upon aging (**Figure S7j-l** and **Supplementary Table 3**). Almost all HSCs express Notch2 (**Figure S7b**) and, accordingly, most Jag2$^+$ HSCs co-express Notch2. Conversely, few HSCs express Notch1, whose expression is not changed upon aging nor upon SECJag2KO (**Figure 6e**, **Figure S7m-n** and **Supplementary Table 3**), and even fewer HSCs (3,01%) co-express Notch1 and Jag2. By iFAST3D histology, we confirmed that Notch2 and Jag2 expression completely overlaps in aged HSCs and that Notch2 and Jag2 co-localize in aged HSCs that are in clusters (**Figure 6f**). Since we observed that in aged *Hes1p-2dEGFP* mice HSC clustering is mainly affecting Notch inactive HSCs (**Figure 5f-h**), we reasoned that Jag2-Notch2 co-expression in HSCs might lead to cis-inhibition of Notch signaling. To test this hypothesis, we applied SigHotSpotter[37] to estimate signaling activation in young and aged Jag2$^+$ vs Jag2$^-$ HSCs. SigHotSpotter identifies hotspots of signaling pathways which are involved in the sustained transmission of external niche signals responsible for the stable maintenance of cell subpopulation phenotypes and functions by integrating signaling and transcriptional networks[37]. Remarkably, SigHotSpotter identified Notch2 signaling activation in Jag2$^-$ HSCs, together with Bmpr2 and a few other pathways (**Figure 6g-h**). Jag2$^+$ HSCs showed low probability of Notch2 activation (meaning that Notch2 is likely inactive), while displaying high probability of active Vwf, Tgfβ1, and Rock2 signaling among others. None of the signaling pathways active in Jag2$^+$ HSCs has been previously associated with Notch signaling inhibition (**Figure 6g-i** and **Supplementary Table 4**). Overall, we conclude that Jag2$^+$ HSCs show significant enrichment for aging, low-output and myeloid-biased signatures, and display Notch2 inactive signaling likely induced by Jag2 cis-inhibition of Notch2 activity.

To further strengthen our conclusion, we tested Jag2 expression in aged *Hes1p-2dEGFP* mice. Noteworthy, most aged Notch inactive HSCs express Jag2, supporting that Jag2 cis-inhibits Notch as suggested by the SigHotSpotter results (**Figure 7a-b**). Moreover, Notch inactive aged Jag2^{+} HSCs also display a reduction in the minimum distance between them and an increased clustering compared to the Jag2 negative counterpart, suggesting that Jag2 expression in aged HSCs might also promote HSC clustering (**Figure 7c-e**). To demonstrate that Jag2 expression in HSCs is necessary for HSC clustering and expansion, we transplanted BM cells isolated from Rosa26Cre^{ERt2} Jag2$^{fl/fl}$ mice into WT CTRL or SEC Jag2KO recipients inducing the contemporary deletion of Jag2 in HSCs and in SECs 6 weeks after transplantation (**Figure 7f**). iFAST3D analysis 7 days after the induction of Jag2 deletion in both HSCs and SECs demonstrated that Jag2 deletion in HSCs counteracts the increase in HSCs frequency and clustering, which is triggered by SEC Jag2KO (**Figure 7g-i**). Collectively, we conclude that Jag2 expression in HSCs is necessary to induce HSC expansion and clustering.

In conclusion the absence of sinusoidal Jag2 leads to an increase in Jag2 expression in HSCs that cis-inhibits Notch signaling promoting HSC clustering upon aging (**Figure 6j**).

Discussion

Notch signaling in hematopoiesis has been largely investigated during embryonic development, while data supporting the relevance of Notch signaling for adult hematopoiesis remains controversial[4,57–60]. Here, we reveal an unexpected role of Notch signaling in preserving the regenerative potential of HSCs upon aging. Our data shows that Notch signaling activation is not homogeneous within the adult HSC pool and depends on HSC localization in proximity to Jag2^{+} SECs. The non-homogeneous Notch activation in adult HSCs reflects the heterogeneity of the adult HSC pool and reveals that Jag2 trans-activation of Notch signaling in HSC depends on the vascular

niche since development to adulthood[31–33,61–64]. In SEC^{Jag2KO} mice, HSC quiescence and differentiation priming are altered, Notch inactive HSCs increase in number, H4K16ac polarity decreases, and symmetric divisions are more frequent, resulting in expansion and clustering of My-HSCs, paralleled by impaired hematopoietic regeneration (**Figure 7j**). Moreover, upon sinusoidal Jag2 deletion, HSC functional impairment persists upon serial transplantations in wild-type recipients, supporting that an extrinsic change in the niche can induce a long-term HSC intrinsic alteration, as reported previously for other BM stroma cells[65]. In agreement with the previously reported decrease of Jag2 expression in aged Nes-GFP^{high} cells and at arteriolar endothelial BM cells, the fraction of Notch inactive HSCs expands upon aging. Aged Notch inactive HSCs localize far away from sinusoids and are found in clusters[16].

Moreover, our data contributes by revealing that Notch trans-activation persists in the subset of aged HSCs close to and dependent on sinusoidal-Jag2 stimulation, while it is lost in the fraction of My-HSCs that in the absence of sinusoidal Jag2 expands and clusters, contributing to the microanatomical remodeling of the aged BM niche[21,22,66] and overall affecting the regenerative capacity of the aged hematopoietic system[67]. It has been shown that aged ECs impair the repopulating capacity of young HSCs imposing a myeloid bias. On the contrary, young ECs restored the repopulating capacity of aged HSCs enhancing hematopoietic recovery following myelosuppressive injury or transplantation, even if they were unable to reverse the intrinsic myeloid bias[15]. Our data mechanistically explains this previous observation and reconciles the apparent discrepancy between extrinsic and intrinsic regulation of HSC aging by revealing that the reduction of sinusoidal Jag2 alters HSC priming and function and induces the expression of Jag2 in My-HSCs, which expand, cluster and are differentiation impaired.

Furthermore, our data agrees with previous reports demonstrating that Notch2 activity induces the expression of genes that impede myeloid differentiation, enhancing the self-renewal of HSCs

and preventing their depletion caused by rapid differentiation[68]. Consistently, here we show that Notch inactivation increases myeloid fate priming and decreases the regenerative capacity of HSCs. Further, we expand on this point by showing that Notch inactive HSCs upregulate Jag2 and maintain an impaired regenerative capacity upon serial transplantation in Jag2 competent (wild type) mice. This reduced ability to receive signals from signaling sending cells while expressing both Notch ligand and receptor is fulfilling the criteria that defines cis-inhibition[69] and in our context this may help explain, at least in part, the reduced regenerative capacity of aged HSCs when transplanted in young niches. Importantly, our data highlights the critical role of precise Notch regulation in aged HSCs, while not excluding the involvement of other Notch regulatory mechanisms in Notch active HSCs, such as lateral inhibition. Further investigation into this aspect could provide valuable insights into how these mechanisms shape the architecture of HSPC differentiation[69,70].

During embryonic development Notch signaling is oscillatory in various systems and these oscillations are essential to determine cell fate, indicating the necessity of a fine balance in the regulation of Notch signaling activation in different cells and in the same cell over time[71]. In the embryo, Notch signaling trans-activation is necessary for HSC emergence. However, Notch activity needs to be dampened once HSCs have been specified and this is achieved by a Jag1-driven cis-inhibitory signal in emergent HSCs[33]. Now our data show that in response to the reduction of endothelial Jag2 in the aged BM vasculature, HSCs switch from a niche-driven extrinsic Notch trans-activation to an intrinsic Jag2 cis-inhibition to block differentiation, resembling what happens during development, where Notch cis-inhibition arrests differentiation of nascent HSCs[33,72]. However, upon aging this Notch trans-activation to cis-inhibition switch plays an antagonistic pleiotropic effect by blocking HSCs in clusters, ultimately impairing aged HSC regenerative capacity (**Figure 7j**). Notch signaling cross talks with several signaling pathways, and we cannot

exclude that this occurs also upon HSC aging. However, in Jag2^{+} HSCs we were unable to identify the occurrence of any signaling crosstalk previously associated with Notch inhibition. In fact, while SigHotSpotter analysis detected high probability of Notch2 activity in Jag2^{-} HSCs, the same signal network analysis identified several other active signaling pathways in Jag2^{+} HSCs, including TGF-β1 and Vwf, previously associated with myeloid bias[73,74]. However, none of the signaling pathways found active in Jag2^{+} HSCs has been previously reported to inhibit Notch signaling, supporting Jag2 cis-inhibition (**Figure 6g-i** and **Supplementary Table 4**).

Collectively, we demonstrate a key role of Notch signaling for adult HSCs. We show that the reduction of sinusoidal Jag2 expression underlies a switch from Notch trans-activation to cis-inhibition in aged HSCs, shifting HSC fate commitment upon division for a subset of stem cells from an extrinsic to an intrinsic driven regulation. Furthermore, we highlight the existence of an unexpected antagonistic pleiotropy of Notch signaling upon HSC aging, which favors the expansion of My-HSCs at the expense of hematopoietic differentiation and regeneration. Finally, we demonstrate that a Notch signaling-mediated crosstalk between extrinsic BM signals and HSC intrinsic features contributes to the maintenance of HSC regenerative capacity throughout life. This finding might extend to other tissues that depend on Notch signaling to regulate somatic stem cell activity for regeneration and aging and might as well be relevant to human HSC aging and regenerative medicine applications, since a similar phenotypic expansion of HSCs has been reported in healthy elderly bone marrow donors.

Acknowledgments

We acknowledge support from Dr. Mercè Marti Gaudes, head of Technical Facilities at IDIBELL together with José Andres Vaquero (IDIBELL FACS and Flow cytometry SCT), Antoni Ventura,

Juana Fernandez Rodriguez, Aida López Fernández (IDIBELL Mouse Facility SCT), Joan Repulles, Saioa Mendizuri and Jaume Boix Fabrés (IDIBELL Bioimaging SCT). We thank Esther Castaño, Beatriz Barroso and Benjamin Torrejon (CCiT-UB, Bellvitge). We thank Arnau Lagarda Tous (Biostatistic Unit of IDIBELL) for advising and revising the statistics all over the manuscript. We thank the Irradiation Unit of ICO for the support with mice irradiation. We thank Ryoichiro Kageyama (Kyoto University, Japan) for generously providing *Hes1p-2dEGFP* mice. We thank Hirotake Ichise (University of Ryukyus, Japan) for generously sharing VEGFR3Cre^{Mer} mice. We thank Jose Luis de La Pompa (CNIC, Madrid) and Thomas Gridley (The Jackson Laboratory, Bar Harbor, USA) for generously sharing Jag2*fl/fl* mice. We thank Alejo Rodriguez-Fraticelli and Indranil Singh (IRB, Barcelona, Spain) for generously sharing *Fgd5ZsGreen-mTdTomato* mice. mice. We thank Gloria Zambelli for the constructive suggestions. We thank Conxi Lazaro (LCAM laboratory, ICO-HUB) for supporting sequencing experiments. We thank CERCA Program/Generalitat de Catalunya for institutional support. We acknowledge the funding sources: European Research Council (ERC) grant 101002453 (MCF) and LaCaixa Health Research grant HR20-00800 (MCF), Department of Research and University of the Generalitat of Catalunya and AGAUR (expedient 2021 SGR 00888) (MCF) and Agencia Estatal de Investigación (AEI), grant PID2022-137945OB-I00 (AB).

Authorship contributions

Conceptualization: FM, MCF

Methodology: FM, SM-V, EM-R, AF-P, DE-J, JL-B, PH-M, RT, JG-M, AB, SJ, AD-M

Investigation: FM, SM-V, MCF

Visualization: FM, PH-M, RT

Funding acquisition: MCF

Project administration: MCF

Supervision: AB, MCF

Writing – original draft: FM, SM-V, MCF

Writing – review & editing: FM, AB, MCF

Disclosure of conflict of interest

The authors declare no competing interests.

References

1. Kasbekar M, Mitchell CA, Proven MA, Passegué E. Hematopoietic stem cells through the ages: A lifetime of adaptation to organismal demands. *Cell Stem Cell*. 2023;30(11):1403-1420. doi:10.1016/j.stem.2023.09.013

2. Geiger H, de Haan G, Florian MC. The ageing haematopoietic stem cell compartment. *Nat Rev Immunol*. 2013;13(5):376-389. doi:10.1038/nri3433

3. Mejia-Ramirez E, Florian MC. Understanding intrinsic hematopoietic stem cell aging. *Haematologica*. 2020;105(1):22-37. doi:10.3324/haematol.2018.211342

4. Thambyrajah R, Bigas A. Notch Signaling in HSC Emergence: When, Why and How. *Cells*. 2022;11(3):358. doi:10.3390/cells11030358

5. Rossi DJ, Bryder D, Zahn JM, et al. Cell intrinsic alterations underlie hematopoietic stem cell aging. *Proc Natl Acad Sci*. 2005;102(26):9194-9199. doi:10.1073/pnas.0503280102

6. Beerman I, Bhattacharya D, Zandi S, et al. Functionally distinct hematopoietic stem cells modulate hematopoietic lineage potential during aging by a mechanism of clonal expansion. *Proc Natl Acad Sci U S A*. 2010;107(12):5465-5470. doi:10.1073/pnas.1000834107

7. Pinho S, Frenette PS. Haematopoietic stem cell activity and interactions with the niche. *Nat Rev Mol Cell Biol*. 2019;20(5):303-320. doi:10.1038/s41580-019-0103-9

8. Ho YH, Méndez-Ferrer S. Microenvironmental contributions to hematopoietic stem cell aging. *Haematologica*. 2020;105(1):38-46. doi:10.3324/haematol.2018.211334

9. Matteini F, Mulaw MA, Florian MC. Aging of the Hematopoietic Stem Cell Niche: New Tools to Answer an Old Question. *Front Immunol*. 2021;12:738204. doi:10.3389/fimmu.2021.738204

10. May M, Slaughter A, Lucas D. Dynamic regulation of hematopoietic stem cells by bone marrow niches. *Curr Stem Cell Rep*. 2018;4(3):201-208. doi:10.1007/s40778-018-0132-x

11. Lucas D. Structural organization of the bone marrow and its role in hematopoiesis. *Curr Opin Hematol*. 2021;28(1):36-42. doi:10.1097/MOH.0000000000000621

12. Young K, Eudy E, Bell R, et al. Decline in IGF1 in the bone marrow microenvironment initiates hematopoietic stem cell aging. *Cell Stem Cell*. 2021;28(8):1473-1482.e7. doi:10.1016/j.stem.2021.03.017

13. Purton LE, Scadden DT. The hematopoietic stem cell niche. Published online 2008. doi:NBK27051 [bookaccession]

14. Batsivari A, Haltalli MLR, Passaro D, Pospori C, Lo Celso C, Bonnet D. Dynamic responses of the haematopoietic stem cell niche to diverse stresses. *Nat Cell Biol*. 2020;22(1):7-17. doi:10.1038/s41556-019-0444-9

15. Poulos MG, Ramalingam P, Gutkin MC, et al. Endothelial transplantation rejuvenates aged hematopoietic stem cell function. *J Clin Invest*. 2017;127(11):4163-4178. doi:10.1172/JCI93940

16. Sacma M, Pospiech J, Bogeska R, et al. Haematopoietic stem cells in perisinusoidal niches are protected from ageing. *Nat Cell Biol*. 2019;21(11):1309-1320. doi:10.1038/s41556-019-0418-y

17. Maryanovich M, Zahalka AH, Pierce H, et al. Adrenergic nerve degeneration in bone marrow drives aging of the hematopoietic stem cell niche. *Nat Med*. 2018;24(6):782-791. doi:10.1038/s41591-018-0030-x

18. Ho YH, Del Toro R, Rivera-Torres J, et al. Remodeling of Bone Marrow Hematopoietic Stem Cell Niches Promotes Myeloid Cell Expansion during Premature or Physiological Aging. *Cell Stem Cell*. 2019;25(3):407-418.e6. doi:10.1016/j.stem.2019.06.007

19. Florian MC, Klose M, Sacma M, et al. Aging alters the epigenetic asymmetry of HSC division. *PLoS Biol*. 2018;16(9):e2003389. doi:10.1371/journal.pbio.2003389

20. Florian MC, Nattamai KJ, Dorr K, et al. A canonical to non-canonical Wnt signalling switch in haematopoietic stem-cell ageing. *Nature*. 2013;503(7476):392-396. doi:nature12631 [pii] 10.1038/nature12631

21. Wu Q, Zhang J, Kumar S, et al. Resilient anatomy and local plasticity of naive and stress haematopoiesis. *Nature*. 2024;627(8005):839-846. doi:10.1038/s41586-024-07186-6

22. Florian MC. Powerful microscopy reveals blood-cell production in bone marrow. *Nature*. Published online 20 March 2024. doi:10.1038/d41586-024-00504-y

23. Vázquez-Ulloa E, Lin KL, Lizano M, Sahlgren C. Reversible and bidirectional signaling of notch ligands. *Crit Rev Biochem Mol Biol*. 2022;57(4):377-398. doi:10.1080/10409238.2022.2113029

24. Kovall RA, Gebelein B, Sprinzak D, Kopan R. The Canonical Notch Signaling Pathway: Structural and Biochemical Insights into Shape, Sugar, and Force. *Dev Cell*. 2017;41(3):228-241. doi:10.1016/j.devcel.2017.04.001

25. Pajcini KV, Speck NA, Pear WS. Notch signaling in mammalian hematopoietic stem cells. *Leukemia*. 2011;25(10):1525-1532. doi:10.1038/leu.2011.127

26. Souilhol C, Lendinez JG, Rybtsov S, et al. Developing HSCs become Notch independent by the end of maturation in the AGM region. *Blood*. 2016;128(12):1567-1577. doi:10.1182/blood-2016-03-708164

27. Boisset JC, van Cappellen W, Andrieu-Soler C, Galjart N, Dzierzak E, Robin C. In vivo imaging of haematopoietic cells emerging from the mouse aortic endothelium. *Nature*. 2010;464(7285):116-120. doi:10.1038/nature08764

28. de Bruijn MFTR, Ma X, Robin C, Ottersbach K, Sanchez MJ, Dzierzak E. Hematopoietic stem cells localize to the endothelial cell layer in the midgestation mouse aorta. *Immunity*. 2002;16(5):673-683. doi:10.1016/s1074-7613(02)00313-8

29. Taoudi S, Medvinsky A. Functional identification of the hematopoietic stem cell niche in the ventral domain of the embryonic dorsal aorta. *Proc Natl Acad Sci U S A*. 2007;104(22):9399-9403. doi:10.1073/pnas.0700984104

30. Mascarenhas MI, Parker A, Dzierzak E, Ottersbach K. Identification of novel regulators of hematopoietic stem cell development through refinement of stem cell localization and expression profiling. *Blood*. 2009;114(21):4645-4653. doi:10.1182/blood-2009-06-230037

31. Guo P, Poulos MG, Palikuqi B, et al. Endothelial jagged-2 sustains hematopoietic stem and progenitor reconstitution after myelosuppression. *J Clin Invest*. Published online 23 October 2017. doi:10.1172/JCI92309

32. Poulos MG, Guo P, Kofler NM, et al. Endothelial Jagged-1 is necessary for homeostatic and regenerative hematopoiesis. *Cell Rep*. 2013;4(5):1022-1034. doi:10.1016/j.celrep.2013.07.048

33. Thambyrajah R, Maqueda M, Neo WH, et al. Cis inhibition of NOTCH1 through JAGGED1 sustains embryonic hematopoietic stem cell fate. *Nat Commun*. 2024;15(1):1604. doi:10.1038/s41467-024-45716-y

34. Ichise T, Yoshida N, Ichise H. FGF2-induced Ras-MAPK signalling maintains lymphatic endothelial cell identity by upregulating endothelial-cell-specific gene expression and suppressing TGFbeta signalling through Smad2. *J Cell Sci*. 2014;127(Pt 4):845-857. doi:10.1242/jcs.137836

35. Xu J, Krebs LT, Gridley T. Generation of mice with a conditional null allele of the Jagged2 gene. *Genes N Y N 2000*. 2010;48(6):390-393. doi:10.1002/dvg.20626

36. Saçma M, Matteini F, Mulaw MA, et al. Fast and high-fidelity in situ 3D imaging protocol for stem cells and niche components for mouse organs and tissues. *STAR Protoc*. 2022;3(3):101483. doi:10.1016/j.xpro.2022.101483

37. Ravichandran S, Hartmann A, del Sol A. SigHotSpotter: scRNA-seq-based computational tool to control cell subpopulation phenotypes for cellular rejuvenation strategies. *Bioinformatics*. 2020;36(6):1963-1965. doi:10.1093/bioinformatics/btz827

38. García-Prat L, Perdiguero E, Alonso-Martín S, et al. FoxO maintains a genuine muscle stem-cell quiescent state until geriatric age. *Nat Cell Biol*. Published online 26 October 2020:1-12. doi:10.1038/s41556-020-00593-7

39. Imayoshi I, Isomura A, Harima Y, et al. Oscillatory control of factors determining multipotency and fate in mouse neural progenitors. *Science*. 2013;342(6163):1203-1208. doi:10.1126/science.1242366

40. Sueda R, Kageyama R. Regulation of active and quiescent somatic stem cells by Notch signaling. *Dev Growth Differ*. 2020;62(1):59-66. doi:10.1111/dgd.12626

41. Guiu J, Shimizu R, D'Altri T, et al. Hes repressors are essential regulators of hematopoietic stem cell development downstream of Notch signaling. *J Exp Med*. 2013;210(1):71-84. doi:10.1084/jem.20120993

42. Thambyrajah R, Bigas A. Notch Signaling in HSC Emergence: When, Why and How. *Cells*. 2022;11(3):358. doi:10.3390/cells11030358

43. Florian MC, Dorr K, Niebel A, et al. Cdc42 activity regulates hematopoietic stem cell aging and rejuvenation. *Cell Stem Cell*. 2012;10(5):520-530. doi:S1934-5909(12)00172-5 [pii] 10.1016/j.stem.2012.04.007

44. Grigoryan A, Guidi N, Senger K, et al. LaminA/C regulates epigenetic and chromatin architecture changes upon aging of hematopoietic stem cells. *Genome Biol*. 2018;19(1):189. doi:10.1186/s13059-018-1557-3

45. Montserrat-Vazquez S, Ali NJ, Matteini F, et al. Transplanting rejuvenated blood stem cells extends lifespan of aged immunocompromised mice. *Npj Regen Med*. 2022;7(1):1-17. doi:10.1038/s41536-022-00275-y

46. Xu J, Krebs LT, Gridley T. Generation of mice with a conditional null allele of the Jagged2 gene. *Genesis*. 2010;48(6):390-393. doi:10.1002/dvg.20626

47. Gazit R, Mandal PK, Ebina W, et al. Fgd5 identifies hematopoietic stem cells in the murine bone marrow. *J Exp Med*. 2014;211(7):1315-1331. doi:jem.20130428 [pii] 10.1084/jem.20130428

48. Chapple RH, Tseng YJ, Hu T, et al. Lineage tracing of murine adult hematopoietic stem cells reveals active contribution to steady-state hematopoiesis. *Blood Adv*. 2018;2(11):1220-1228. doi:10.1182/bloodadvances.2018016295

49. Gekas C, Graf T. CD41 expression marks myeloid-biased adult hematopoietic stem cells and increases with age. *Blood*. 2013;121(22):4463-4472. doi:10.1182/blood-2012-09-457929

50. Bigas A, Espinosa L. Hematopoietic stem cells: to be or Notch to be. *Blood*. 2012;119(14):3226-3235. doi:10.1182/blood-2011-10-355826

567 51. Balistreri CR, Madonna R, Melino G, Caruso C. The emerging role of Notch pathway in ageing: Focus on
568 the related mechanisms in age-related diseases. *Ageing Res Rev*. 2016;29:50-65.
569 doi:10.1016/j.arr.2016.06.004

570 52. Mejia-Ramirez E, Picazo-Ianez P, Montserrat-Vazquez, Sara, et al. Targeting RhoA activity rejuvenates
571 aged haematopoietic stem cells by reducing nuclear stretching. *Revis*. Published online 2025.

572 53. Hao Y, Hao S, Andersen-Nissen E, et al. Integrated analysis of multimodal single-cell data. *Cell*.
573 2021;184(13):3573-3587.e29. doi:10.1016/j.cell.2021.04.048

574 54. Flohr Svendsen A, Yang D, Kim K, et al. A comprehensive transcriptome signature of murine
575 hematopoietic stem cell aging. *Blood*. 2021;138(6):439-451. doi:10.1182/blood.2020009729

576 55. Rodriguez-Fraticelli AE, Weinreb C, Wang SW, et al. Single-cell lineage tracing unveils a role for TCF15 in
577 haematopoiesis. *Nature*. 2020;583(7817):585-589. doi:10.1038/s41586-020-2503-6

578 56. Mann M, Mehta A, de Boer CG, et al. Heterogeneous Responses of Hematopoietic Stem Cells to
579 Inflammatory Stimuli are Altered with Age. *Cell Rep*. 2018;25(11):2992-3005.e5.
580 doi:10.1016/j.celrep.2018.11.056

581 57. Maillard I, Koch U, Dumortier A, et al. Canonical notch signaling is dispensable for the maintenance of
582 adult hematopoietic stem cells. *Cell Stem Cell*. 2008;2(4):356-366. doi:10.1016/j.stem.2008.02.011

583 58. Vanderbeck AN, Maillard I. Notch in the niche: new insights into the role of Notch signaling in the bone
584 marrow. *Haematologica*. 2019;104(11):2117-2119. doi:10.3324/haematol.2019.230854

585 59. Butko E, Pouget C, Traver D. Complex regulation of HSC emergence by the Notch signaling pathway. *Dev*
586 *Biol*. 2016;409(1):129-138. doi:10.1016/j.ydbio.2015.11.008

587 60. Lomelí H, Castillo-Castellanos F. Notch signaling and the emergence of hematopoietic stem cells. *Dev*
588 *Dyn Off Publ Am Assoc Anat*. 2020;249(11):1302-1317. doi:10.1002/dvdy.230

589 61. Butler JM, Nolan DJ, Vertes EL, et al. Endothelial cells are essential for the self-renewal and
590 repopulation of Notch-dependent hematopoietic stem cells. *Cell Stem Cell*. 2010;6(3):251-264.
591 doi:10.1016/j.stem.2010.02.001

592 62. Hadland BK, Varnum-Finney B, Poulos MG, et al. Endothelium and NOTCH specify and amplify aorta-
593 gonad-mesonephros-derived hematopoietic stem cells. *J Clin Invest*. 2015;125(5):2032-2045.
594 doi:10.1172/JCI80137

595 63. Zhang YW, Mess J, Aizarani N, et al. Hyaluronic acid-GPRC5C signalling promotes dormancy in
596 haematopoietic stem cells. *Nat Cell Biol*. 2022;24(7):1038-1048. doi:10.1038/s41556-022-00931-x

597 64. Rodriguez-Fraticelli AE, Wolock SL, Weinreb CS, et al. Clonal analysis of lineage fate in native
598 hematopoiesis. *Nature*. 2018;553(7687):212-216. doi:10.1038/nature25168

599 65. Derecka M, Herman JS, Cauchy P, et al. EBF1-deficient bone marrow stroma elicits persistent changes in
600 HSC potential. *Nat Immunol*. 2020;21(3):261-273. doi:10.1038/s41590-020-0595-7

66. Verovskaya EV, Dellorusso PV, Passegué E. Losing Sense of Self and Surroundings: Hematopoietic Stem Cell Aging and Leukemic Transformation. *Trends Mol Med*. 2019;25(6):494-515. doi:10.1016/J.MOLMED.2019.04.006

67. Säwen P, Eldeeb M, Erlandsson E, et al. Murine HSCs contribute actively to native hematopoiesis but with reduced differentiation capacity upon aging. *eLife*. 7:e41258. doi:10.7554/eLife.41258

68. Varnum-Finney B, Halasz LM, Sun M, Gridley T, Radtke F, Bernstein ID. Notch2 governs the rate of generation of mouse long- and short-term repopulating stem cells. *J Clin Invest*. 2011;121(3):1207-1216. doi:10.1172/JCI43868

69. del Álamo D, Rouault H, Schweisguth F. Mechanism and significance of cis-inhibition in Notch signalling. *Curr Biol CB*. 2011;21(1):R40-47. doi:10.1016/j.cub.2010.10.034

70. Sjöqvist M, Andersson ER. Do as I say, Not(ch) as I do: Lateral control of cell fate. *Dev Biol*. 2019;447(1):58-70. doi:10.1016/j.ydbio.2017.09.032

71. Bosman SL, Sonnen KF. Chapter Nine - Signaling oscillations in embryonic development. In: Soriano PM, ed. *Current Topics in Developmental Biology*. Vol 149. Cell Signaling Pathways in Development. Academic Press; 2022:341-372. doi:10.1016/bs.ctdb.2022.02.011

72. Souilhol C, Lendinez JG, Rybtsov S, et al. Developing HSCs become Notch independent by the end of maturation in the AGM region. *Blood*. 2016;128(12):1567-1577. doi:10.1182/blood-2016-03-708164

73. Wang X, Dong F, Zhang S, et al. TGF-β1 Negatively Regulates the Number and Function of Hematopoietic Stem Cells. *Stem Cell Rep*. 2018;11(1):274-287. doi:10.1016/j.stemcr.2018.05.017

74. Pinho S, Marchand T, Yang E, Wei Q, Nerlov C, Frenette PS. Lineage-Biased Hematopoietic Stem Cells Are Regulated by Distinct Niches. *Dev Cell*. 2018;44(5):634-641 e4. doi:10.1016/j.devcel.2018.01.016

75. Cabezas-Wallscheid N, Buettner F, Sommerkamp P, et al. Vitamin A-Retinoic Acid Signaling Regulates Hematopoietic Stem Cell Dormancy. *Cell*. 2017;169(5):807-823.e19. doi:10.1016/j.cell.2017.04.018

76. Mejía-Ramírez E, Picazo PI, Walter B, et al. Targeting RhoA activity rejuvenates aged hematopoietic stem cells. Published online 23 April 2025:2025.04.23.647902. doi:10.1101/2025.04.23.647902

77. Hao Y, Stuart T, Kowalski MH, et al. Dictionary learning for integrative, multimodal and scalable single-cell analysis. *Nat Biotechnol*. 2024;42(2):293-304. doi:10.1038/s41587-023-01767-y

78. Kowalczyk MS, Tirosh I, Heckl D, et al. Single cell RNA-seq reveals changes in cell cycle and differentiation programs upon aging of hematopoietic stem cells. *Genome Res*. Published online 1 October 2015. doi:gr.192237.115 [pii] 10.1101/gr.192237.115

79. Choudhary S, Satija R. Comparison and evaluation of statistical error models for scRNA-seq. *Genome Biol*. 2022;23(1):1-20. doi:10.1186/s13059-021-02584-9

80. Wilson NK, Kent DG, Buettner F, et al. Combined Single-Cell Functional and Gene Expression Analysis Resolves Heterogeneity within Stem Cell Populations. *Cell Stem Cell*. 2015;16(6):712-724. doi:10.1016/j.stem.2015.04.004

636 81. Finak G, McDavid A, Yajima M, et al. MAST: a flexible statistical framework for assessing transcriptional
637 changes and characterizing heterogeneity in single-cell RNA sequencing data. *Genome Biol*.
638 2015;16(1):1-13. doi:10.1186/s13059-015-0844-5

639 82. Wu T, Hu E, Xu S, et al. clusterProfiler 4.0: A universal enrichment tool for interpreting omics data. *The*
640 *Innovation*. 2021;2(3):100141. doi:10.1016/j.xinn.2021.100141

641

Figure Legends

Figure 1| Notch signaling activation in adult HSCs depends on BM localization and regulates HSC epipolarity.

a) Representative 3D reconstruction of EGFP expression in HSC of adult *Hes1p-2dEGFP* mice as readout of Notch signaling activation. EGFP negative HSCs are labelled Notch INACTIVE while EGFP expressing HSCs as Notch ACTIVE. b) Pie chart showing the percentage of Notch active and inactive HSC in adult young *Hes1p-2dEGFP* mice n=3. c-d) Representative 3D reconstruction of Notch active HSC localization in proximity to sinusoids (c) and arteries (d) Yellow dotted lines highlight the vessel shape and yellow arrowheads point at HSCs. e) Representative 3D reconstruction of HSC distance from the endosteum in dependance of Notch signaling activation. Dotted lines indicate HSC distance from the endosteum, grey and green dots represent respectively Notch inactive and active HSCs. f) HSC distance from sinusoids, arteries and endosteum. Median with 95% CI, Mann-Whitney two tail. Each single point is the measurement of the distance of single HSC from the analyzed niche compartment, biological n=3. g) Representative 3D reconstruction of H4K16ac polar and apolar distribution in HSCs. h-i) Percentage of H4K16ac polarity in Notch active and inactive HSCs in adult young *Hes1p-2dEGFP* mice by iFAST3D. Pie chart (h) n=3. Bar plot (i) shows mean±SEM, Unpaired t-test one tail, n=3. See also Figure S1-S2.

Figure 2| Sinusoidal Jag2 deletion reduces HSC regenerative capacity after myeloproliferative stress and decreases Notch signaling activation in HSCs.

a) Cartoon scheme representing the mouse model used to selectively delete Jag2 from the sinusoidal compartment. Created with BioRender.com. b) Schematic representation of 5FU

treatment in SEC Jag2KO mice and bleeding points. c) Probability of survival after 5FU treatment., Mantel-Cox test. WT CTRL n=8 and SECJag2KO n=10. d), number of white blood cell (WBC), percentage of lymphoid cells, number of monocytes and granulocytes, percentage of myeloid cells, number of red blood cells (RBC) and hemoglobin (HGB) concentration at the analyzed timepoints after 5FU-induced myeloproliferative stress. Mean±SEM. Linear model for single time point analysis and for time-trend analysis, WT CTRL n=8 and SECJag2KO n=10. e) Schematic representation of transplantation of BM cells from *Hes1p-2dEGFP* mice into SEC Jag2KO lethally irradiated recipients. Total BM transplant has been performed by intravenous injection of 2*10^6 total BM cells isolated from *Hes1p-2dEGFP* donor mice into lethally irradiated VEGFR3Cre^{Mer}Jag2*fl/fl* recipients. TAM induction of Jag2 deletion has been obtained by 3 consecutive days of TAM injections 6 week after irradiation. Recipients BM has been analyzed by iFAST3D histology 7 days from the induction of sinusoidal Jag2 deletion. f) Percentage of Notch inactive and inactive HSCs in recipient mice by iFAST3D. Mean±SEM, One-way ANOVA Tukey multiple comparison test, WT CTRL n=3 and SECJag2KO n=3. g) Representative 3D reconstruction of Notch active HSCs in WT CTRL or SEC Jag2KO recipients. Sinusoids are contoured by a dotted blue line while arteries by a dotted yellow line. The upper panel shows a Notch active HSCs (green EGFP+ HSCs) in WT CTRLs residing near sinusoids while the lower panel shows a Notch active HSC residing close to an artery but far from a sinusoid. h) Minimum distance from the closest sinusoid of Notch inactive and inactive HSCs in recipient mice. Median with 95% CI, Kruskal-Wallis two tail Dunn's multiple analysis test. Each single point is the measurement of the distance of single HSC from sinusoids, biological n: WT CTRL n=3 and SECJag2KO n=3. i) Percentage of Notch inactive and inactive HSCs in recipient mice in proximity to sinusoids (distance HSC-vessel<10μm). Mean±SEM, One-way ANOVA Tukey multiple comparison test, WT CTRL n=3. See also Figure S3.

Figure 3| Sinusoidal Jag2 deletion increases HSC frequency and impairs HSC regenerative capacity upon transplantation.

a) Representative 3D reconstruction of HSC frequency in the BM of WT CTRL and SEC Jag2KO mice. b) HSC number in the BM of SEC Jag2KO mice 7 days after TAM induction of sinusoidal Jag2 deletion analyzed by iFAST3D histology. Mean±SEM, Unpaired t-test one tail, WT CTRL n=3 and SEC Jag2KO n=3. c) Percentage of H4K16ac polarity in SECJag2KO compared to WT CTRL mice analyzed by iFAST3D histology 7 days after TAM induction of sinusoidal Jag2 deletion. Mean±SEM, n=3, Unpaired t-test one tail, WT CTRL n=3 and SECJag2KO n=3. d) Representative 3D reconstruction of epipolar HSC localization in WT CTRL and SEC Jag2KO mice 7 days after TAM treatment. Sinusoids are contoured by yellow dotted lines while HSCs by green dotted lines. Pink box highlighted the magnification area containing the HSC. e) Minimum distance from the closest sinusoid and artery of epipolar HSCs in WT CTRL and SEC Jag2KO mice treatment. Median with 95% CI, Mann-Whitney two tail. Each single point is the measurement of the distance of single HSC from sinusoids, biological n: WT CTRL n=3 and SECJag2KO n=3. f) Schematic representation of transplantation of BM cells from WT CTRL or SEC Jag2KO mice into lethally irradiated Cd45.1 recipients. Primary transplantation end point after 22 weeks followed by BM profiling and secondary transplantation into lethally irradiated Cd45.1 recipients for a duration of 20 weeks. Cartoon scheme created with BioRender.com. g) PB engraftment analysis upon primary (Tx_I) and secondary (Tx_II) transplantation. Mean±SEM, Unpaired t-test one tail at each time point. Tx_I: 4 weeks WT CTRL n=12 and SECJag2KO n=12, 8 and 12 weeks WT CTRL n=8 and SECJag2KO n=7 and at 16 weeks WT CTRL n=11 and SECJag2KO n=10; Tx_II : 4 weeks WT CTRL n=8 and SECJag2KO n=8, and 16 weeks WT CTRL n=6 and SECJag2KO n=6. Each dot represents the average value for each time point. Total BM transplant has been performed by intravenous injection of 1*10^6 total BM cells isolated from

donor VEGFR3Cre^{Mer}Jag2*fl/fl* mice mixed with an equal amount of competitor cells into lethally irradiated BoyJ recipients upon primary transplantation. 2*10^6 total BM cells isolated from primary recipients were used for secondary transplantation cells into lethally irradiated BoyJ recipients. h) Percentage of donor-derived engrafted cells in the BM after 20 weeks from primary transplantation. Mean±SEM, Unpaired t-test one tail, WT CTRL n=8 and SEC Jag2KO n=8. Each dot represents a single mouse. i) Percentage of donor-derived LT-HSC, ST-HSC and L-MPP after 20 weeks from primary transplantation. Mean±SEM, Unpaired t-test one tail, WT CTRL n=8 and SEC Jag2KO n=8. Each dot represents a single mouse. j) Percentage of donor-derived engrafted cells in the BM after 20 weeks from secondary transplantation. Mean±SEM, Unpaired t-test one tail, WT CTRL n=6 and SEC Jag2KO n=6. Each dot represents a single mouse. k) Percentage of donor-derived LT-HSC, ST-HSC and L-MPP after 16 weeks from secondary transplantation. Mean±SEM, Unpaired t-test one tail, WT CTRL n=6 and SEC Jag2KO n=6. Each dot represents a single mouse. See also Figure S4.

Figure 4| Sinusoidal Jag2 deletion alters HSC divisional symmetry and priming and reduces HSC differentiation capacity.

a) Schematic representation of the analysis of HSC DP by iFAST3D histology. Cartoon scheme created with BioRender.com. b) Representative 3D reconstruction and main z-plan in 2D of HSC symmetric and asymmetric HSC division. Symmetry or Asymmetry of HSC division is evaluated by H4K16ac amount segregation between the daughter cells. Analysis of H4K16ac amount inheritance in the daughter cells is calculated in 2D (latest panel on the right) on the main z-plane of the DP and is measured (yellow line) perpendicularly to the division plane (dotted grey axis). On the right, analysis of H4K16ac intensity in the daughter cells of the DP separated by the division plane (dotted grey axis). The HSC DP is contoured

by yellow dotted lines and pointed by a yellow arrow. c) Number of DP in WT CTRL and SEC Jag2KO mice. Mean±SEM, Mann-Whitney one tail, WT CTRL n=3 and SEC Jag2KO n=3. d) Number of symmetric and asymmetric DP in WT CTRL and SEC Jag2KO mice. Mean±SEM, Kruskal-Wallis Dunn's multiple test analysis, WT CTRL n=3 and SEC Jag2KO n=3. e) Schematic representation of the transplantation strategy used to transplant Fgd5ZsGreen-tdTomato BM cells into lethally irradiated WT CTRL or SEC Jag2 KO recipients. Total BM transplant has been performed by intravenous injection of 1*10^6 total BM cells isolated from Fgd5ZsGreen-mTdTomato donor mice mixed with an equal amount of competitor cells into lethally irradiated VEGFR3CreMerJag2fl/fl recipients. 6 weeks after transplantation tomato expression and Jag2 deletion were contemporary induce by 3 days of consecutive TAM treatment. BM iFAST3D analysis has been performed 24-28h or 7 days after TAM treatment. Nomenclature of Fgd5ZsGreen-tdTomato donor-derived cells identified. Cartoon scheme created with BioRender.com. f) Representative 3D reconstruction of Fgd5ZsGreen-tdTomato DP 24-28 hours after TAM. The HSC DP is contoured by yellow dotted lines and pointed by a yellow arrow. g) Number of Fgd5zsGreentdTomato derived HSC and My-HSCs. Mean±SEM, Unpaired t-test one tail. WT CTRL n=3 and SECJag2KO n=3. h) Representative 3D reconstruction of donor-derived My-HSC frequency in the BM of WT CTRL and SEC Jag2KO recipients. i) Fold difference of the percentage of HSC and My-HSCs in cluster in WT CTRL and SEC Jag2KO mice. Mean±SEM, Kruskal-Wallis Dunn's multiple test analysis. WT CTRL n=3 and SECJag2KO n=3. j) Number of Fgd5zsGreentdTomato derived cProg. Mean±SEM, Unpaired t-test one tail. WT CTRL n=3 and SECJag2KO n=3. k) Representative 3D reconstruction of donor-derived cProg frequency in the BM of WT CTRL and SEC Jag2KO recipients. l) Donor-derived cells differentiation output in PB upon transplant in WT CTRL or SEC Jag2KO mice. Mean±SEM, Two-way ANOVA. WT CTRL n=5 and SECJag2KO n=4. m) Donor-derived cells T, B and myeloid

cells in PB upon transplant in WT CTRL or SEC Jag2KO mice. Mean±SEM, Two-way ANOVA. WT CTRL n=5 and SECJag2KO n=4.

Figure 5| Notch signaling activation decreases upon aging while Jag2+HSCs and clustering increase.

a) Representative 3D reconstruction of Notch active and inactive cell distribution and frequency in the BM upon aging. b) Number of Notch active and inactive HSCs in young and aged mice. Mean±SEM, One-way ANOVA Tukey's multiple analysis test, young n=3 and aged n=3. c-e) Minimum distance from the closest sinusoid (c), artery (d) and from the endosteum (e) of Notch active and inactive HSC in aged mice. Median with 95% CI, Mann-Whitney two tail, Each single point is the measurement of the distance of single HSC from sinusoids, arteries or endosteum, biological n=3. f) Representative 3D reconstruction of Notch inactive HSC in cluster. HSCs are contoured by a yellow dotted line. g) Percentage of Notch active and inactive HSCs in cluster in young and aged mice. Mean±SEM, One-way ANOVA Tukey's multiple analysis test, young n=3 and aged n=3. h) Minimum distance of Notch active and inactive HSCs from the closest HSC in young and aged mice. Median with 95% CI, Kruskal-Wallis two tail Dunn's multiple analysis test. Each single point is the measurement of the distance of single HSC from the closest HSC, biological n: young n=3 and aged n=3. i) Representative 3D reconstruction of Jag2 expressing HSCs in cluster. HSCs are contoured by a yellow dotted line. j) Percentage of Jag2 expressing (Jag2 positive) and non-expressing (Jag2 negative) HSC in young and aged mice by iFAST3D. Mean±SEM, One-way ANOVA Tukey's multiple analysis test, young n=5 and aged n=5. k) Minimum distance of Jag2 positive and negative HSCs from the closest HSC in young and aged mice. Median with 95% CI, Kruskal-Wallis two tail Dunn's multiple analysis test. Each single point is the measurement of the distance of single HSC from the closest HSC, biological n: young n=5

and aged n=5. l) Percentage of Jag2 positive and Jag2 negative HSCs in cluster in young and aged mice by iFAST3D. Mean±SEM, One-way ANOVA Tukey's multiple analysis test, young n=5 and aged n=5. m) Minimum distance of Jag2 positive and Jag2 negative HSCs from the closest HSC in WT CTRL and SEC Jag2KO mice. Median with 95% CI, Kruskal-Wallis two tail Dunn's multiple analysis test, Each single point is the measurement of the distance of single HSC from the closest HSC, biological n: WT CTRL n=3 and SEC Jag2KO n=3. n) Percentage of Jag2 positive and Jag2 negative HSCs in cluster in WT CTRL and SEC Jag2KO mice. Mean±SEM, One-way ANOVA Tukey's multiple analysis test, WT CTRL n=3 and SEC Jag2KO n=3. o) Number of Jag2 positive and Jag2 negative HSCs in WT CTRL and SEC Jag2KO mice. Mean±SEM, One-way ANOVA Tukey's multiple analysis test, WT CTRL n=3 and SEC Jag2KO n=3. See also Figure S6.

Figure 6| Jag2 expression is linked to Notch signaling cis-inhibition in HSCs.

a) scRNA-seq clustered UMAP of LSKs. HSC: hematopoietic stem cells; MPP: multipotent progenitor cells; LMPP: lymphoid MPP; CMP: common myeloid progenitors; CLP: common lymphoid progenitors. b) Jag2+ and Jag2- cells in the UMAP. c) Differential expression results in Jag2+ vs Jag2- HSCs. Log2FC: logarithmic 2-fold change. Significantly (Bonferroni adjusted p-value < 0.05 and $|\log2FC| > 0.58$) upregulated (green) and downregulated (pink) are shown. Top 6 genes are labelled. Jag2's (triangle) log2FC is out of the margin of the plot. d) GSEA enrichment for gene signatures of HSC aging, low/high-output HSCs, and myeloid-biased HSCs[54,55,75] in Jag2+ *vs* Jag2- HSCs. NES: normalized enrichment score. Green line: significantly positively enriched in Jag2+; pink line: significantly negatively enriched in Jag2+. Permutation test with Benjamini-Hochberg (BH) p-value adjustment. e) Jag2+, Notch2+ and Jag2+Notch2+ cells in the UMAP. f) Representative 3D reconstruction of Jag2 and Notch2 expression in aged HSCs in cluster.

Notch2^{+} Jag2^{+} HSCs are contoured by a light blue dotted line. g) Cleveland plot showing the activation probability determined by SigHotSpotter of the top signaling molecules in Jag2- and Jag2+ HSCs. Molecules with an activation probability of greater than 0.55 in one population and smaller than 0.45 in the other population are considered to be differentially active. h,i) Schematic representation of the signaling networks of (h) Notch2 in Jag2- HSCs and (i) Tgfbr1 in Jag2+ HSCs. Selected signaling cascades are depicted. Solid lines represent direct interactions while dashed lines represent signaling cascades involving multiple proteins.

Figure 7| Jag2 expression in HSCs induces HSC clustering.

a) Number of Jag2 positive and negative HSCs within the Notch inactive fraction of aged HSCs of *Hes1p-2dEGFP* mice. Mean±SEM, Unpaired t-test one tail, n=3. b) Representative 3D reconstruction of Jag2 expressing Notch inactive HSCs in cluster. Notch inactive Jag2^{+} HSCs are contoured by a yellow dotted line. c) Minimum distance of Jag2 positive and Jag2 negative HSCs from the closest HSC within the Notch inactive fraction of aged HSCs of *Hes1p-2dEGFP* mice. Median with 95% CI, Mann-Whitney two tail, Each single point is the measurement of the distance of single HSC from the closest HSC, biological n=3. d) Percentage of Jag2 positive and Jag2 negative HSCs in cluster within the Notch inactive fraction of aged HSCs of *Hes1p-2dEGFP* mice by iFAST3D. Mean±SEM, Unpaired t-test two tail, n=3. e) Percentage of Notch active and Notch inactive HSC withing the Jag2 positive HSCs in cluster of aged HSCs of *Hes1p-2dEGFP* mice by iFAST3D. Mean±SEM, Unpaired t-test one tail, n=3. f) Schematic representation of the transplantation strategy used to transplant Jag2KO BM cells into lethally irradiated WT CTRL or SEC Jag2 KO recipients. 6 weeks after transplantation, Jag2 deletion in donor-derived HSCs and at SECs were contemporary induce by 3 days of consecutive TAM treatment. BM iFAST3D analysis has

been performed 7 days after TAM treatment. Cartoon scheme created with BioRender.com. g) Number of HSCs Jag2 WT and Jag2 KO identified by iFAST3D in WT CTRL and SEC Jag2KO recipients 7 days after TAM treatment. Mean±SEM, One-way ANOVA Tukey's multiple analysis test, WT CTRL n=3 and SEC Jag2KO n=3. h) Percentage of Jag2 WT and Jag2 KO HSCs in cluster identified by iFAST3D in WT CTRL and SEC Jag2KO recipients 7 days after TAM treatment. Mean±SEM, One-way ANOVA Tukey's multiple analysis test, WT CTRL n=3 and SEC Jag2KO n=3 i) Minimum distance of Jag2 WT and Jag2 KO HSCs from the closest HSC in WT CTRL and SEC Jag2KO recipients. Median with 95% CI, Kruskal-Wallis two tail Dunn's multiple analysis test. Each single point is the measurement of the distance of single HSC from the closest HSC, biological n: WT CTRL n=3 and SEC Jag2KO n=3. j) Schematic summary of the described results. Created with BioRender.com.

Figure 1: Notch signaling activation in adult HSCs depends on BM localization and regulates HSC epipolarity

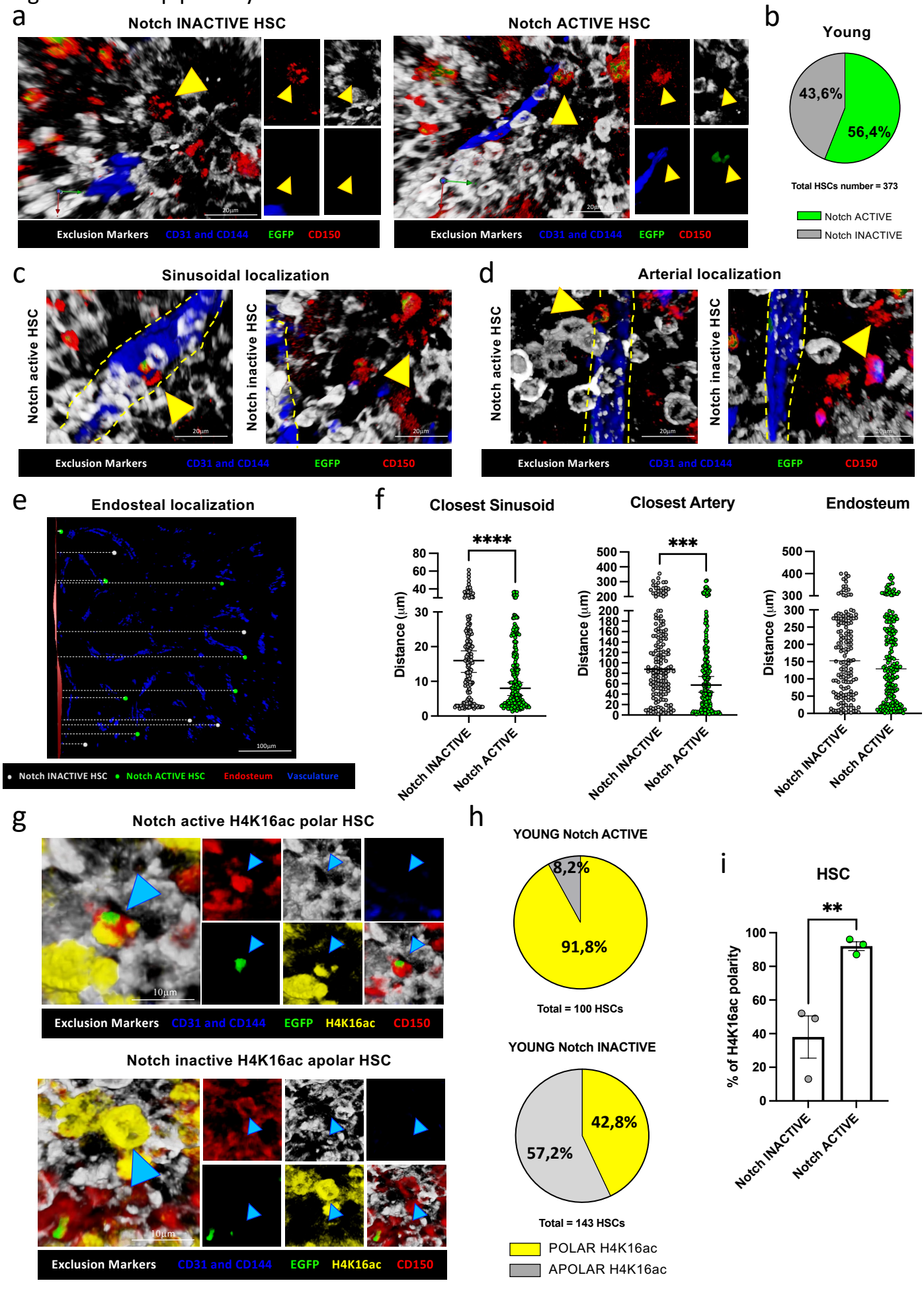

Figure 2: Sinusoidal Jag2 deletion reduces HSC regenerative capacity after myeloproliferative stress and decreases Notch signaling activation in HSCs.

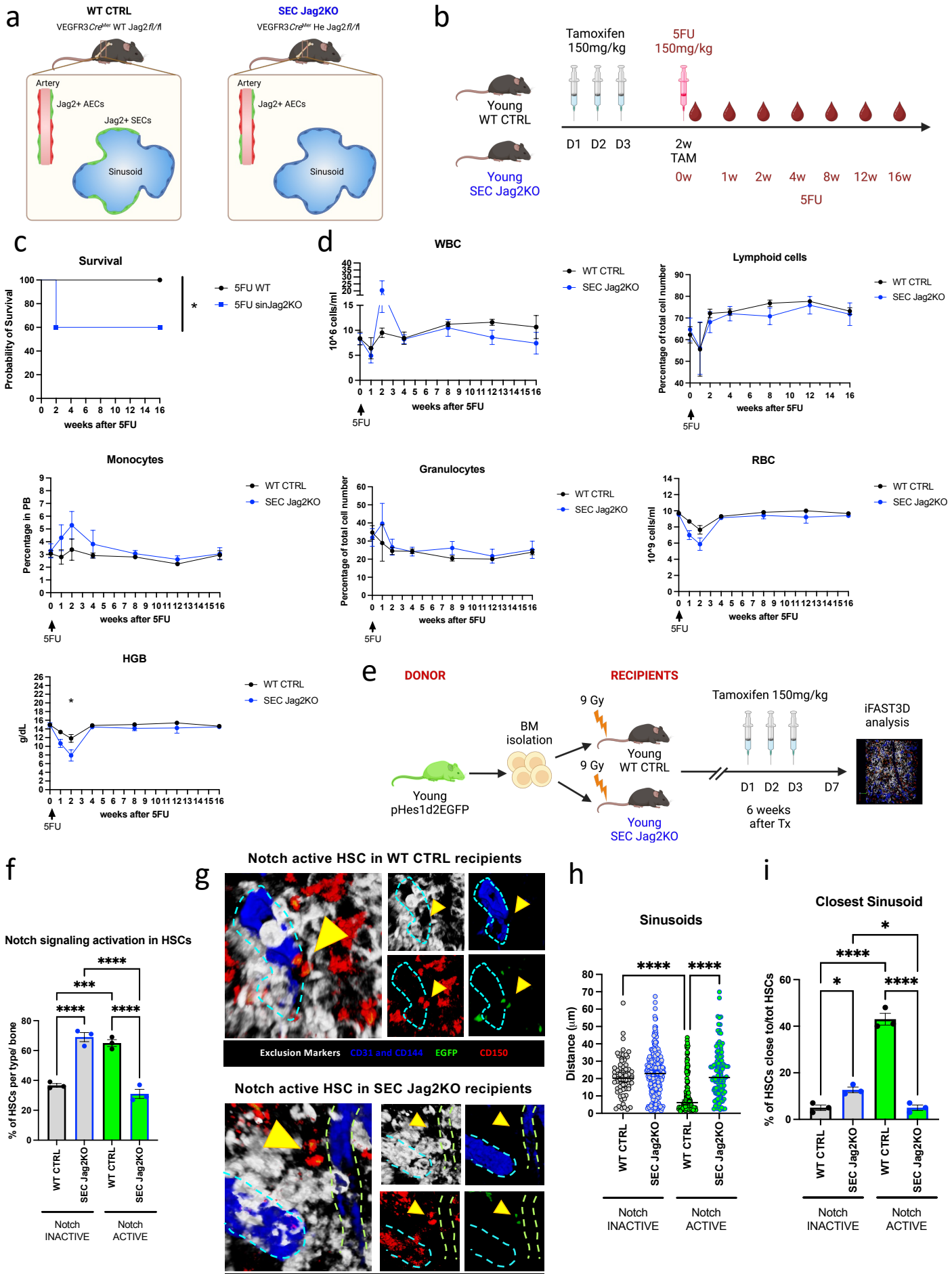

Figure3: Sinusoidal Jag2 deletion increases HSC frequency and impairs HSC regenerative capacity upon transplantation.

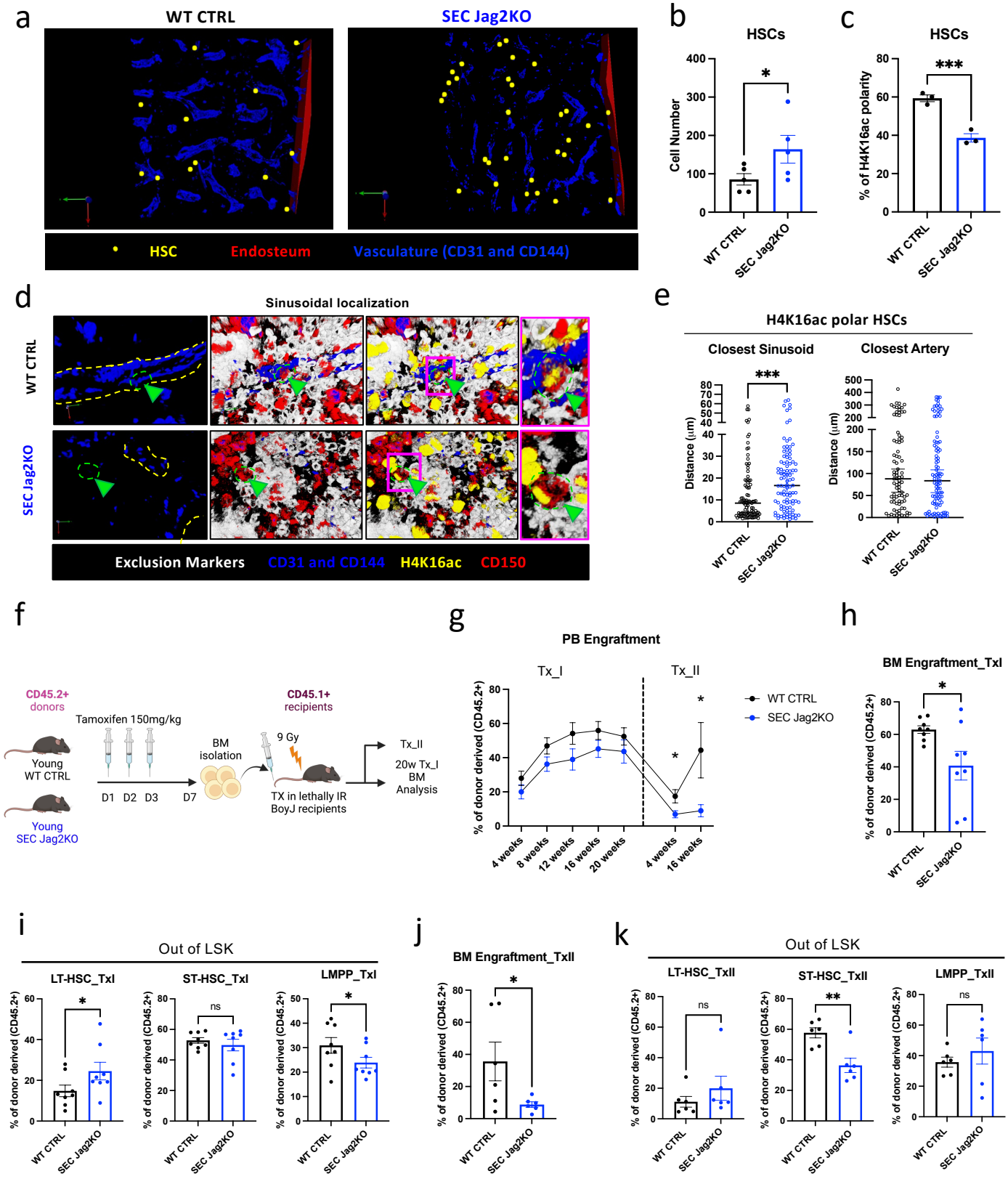

Figure 4: Sinusoidal Jag2 deletion alters HSC divisional symmetry and priming and reduces HSC differentiation capacity.

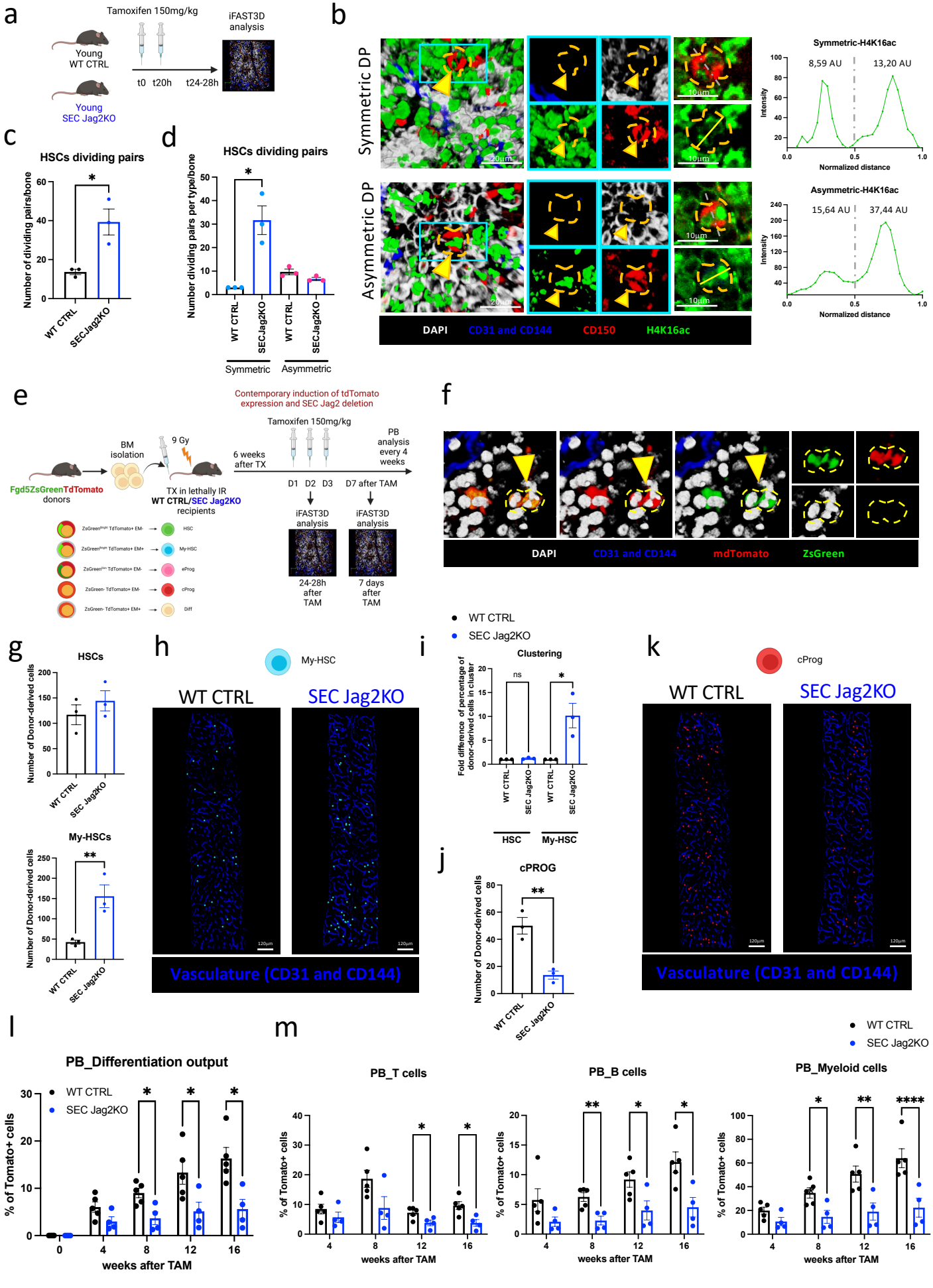

Figure 5: Notch signaling activation decreases upon aging while Jag2+HSCs and clustering increase.

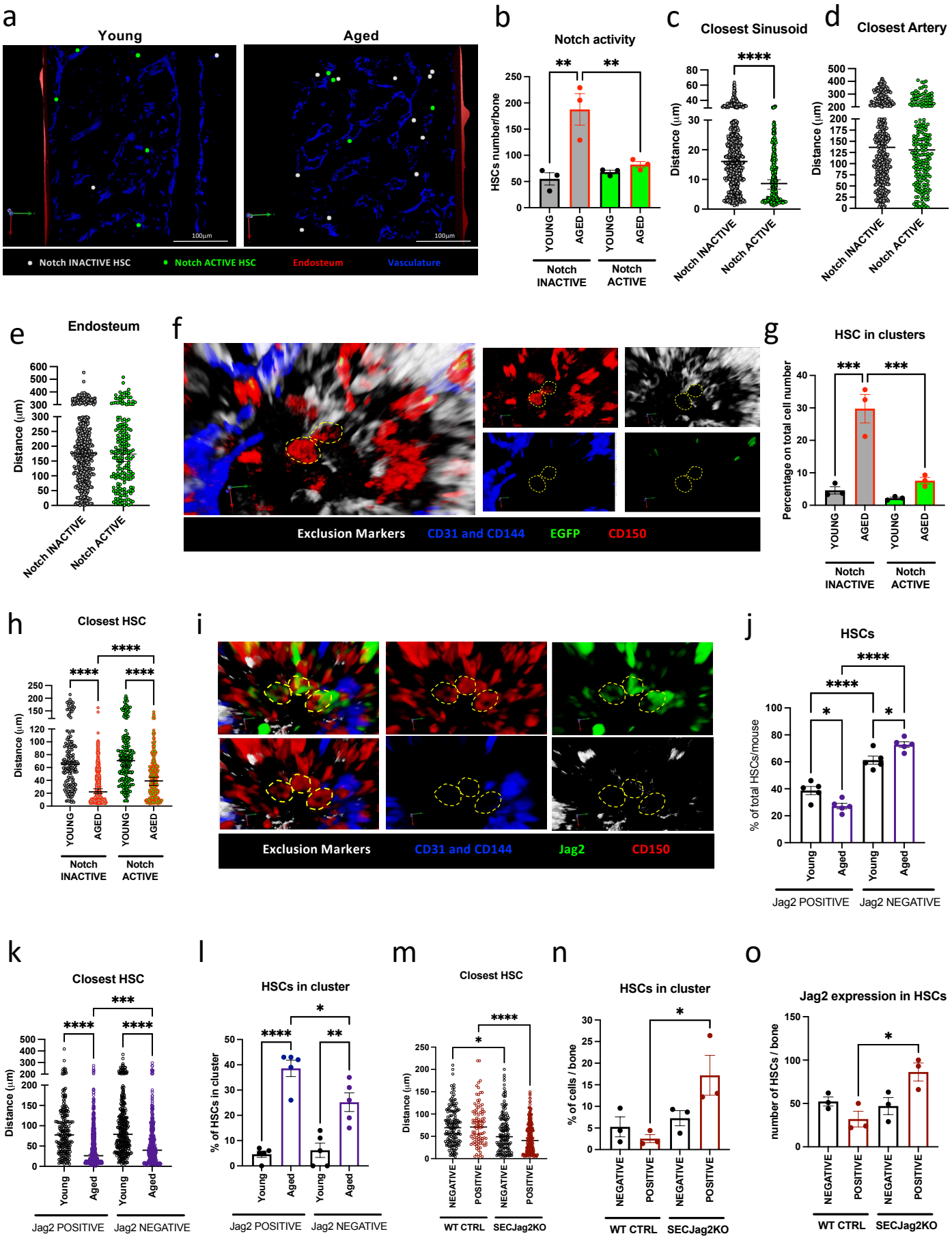

Figure 6: Jag2 expression is linked to Notch signaling inhibition in HSCs.

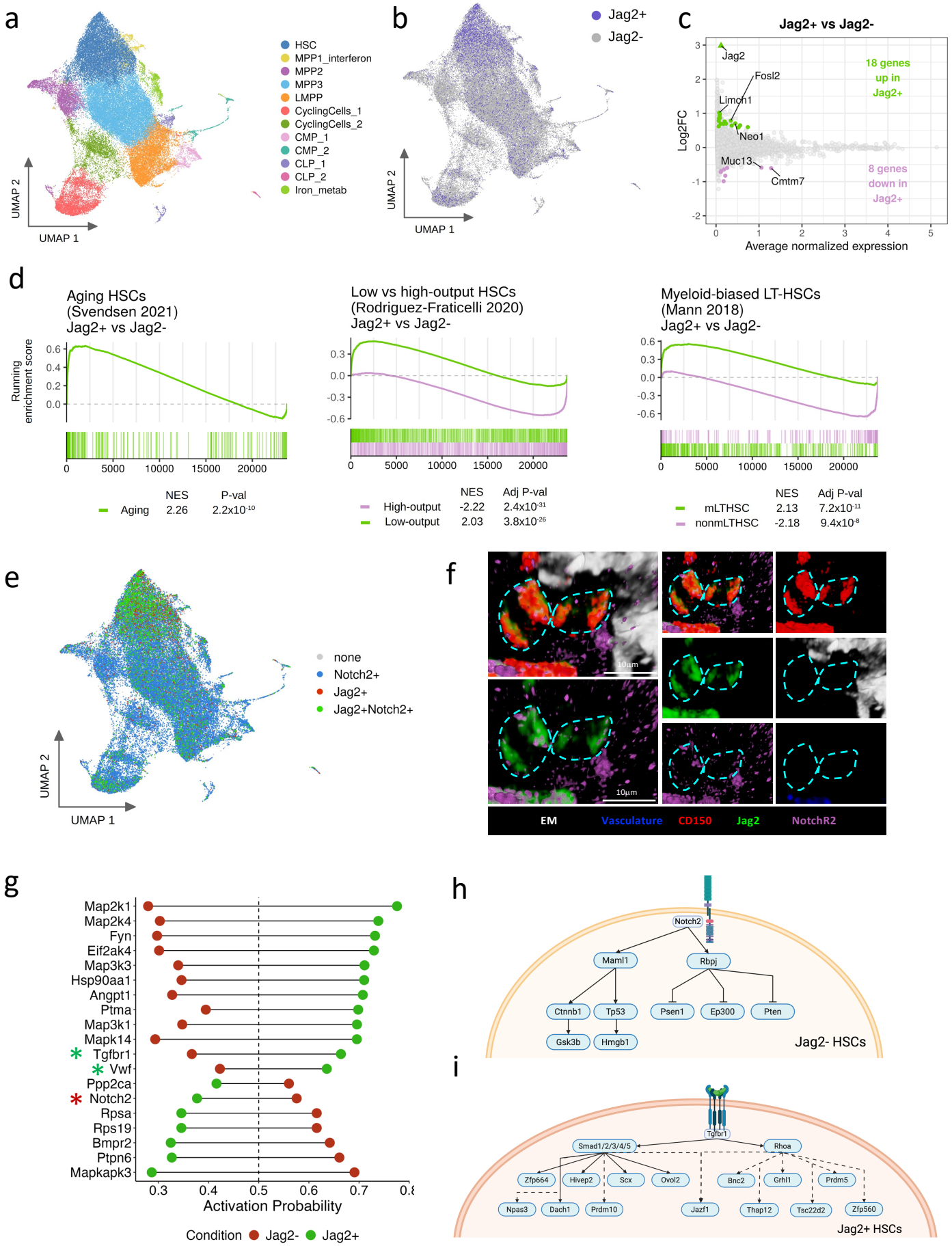

Figure 7: Jag2 expression in HSCs induces HSC clustering.